CHALMERS
UNIVERSITY OF TECHNOLOGY

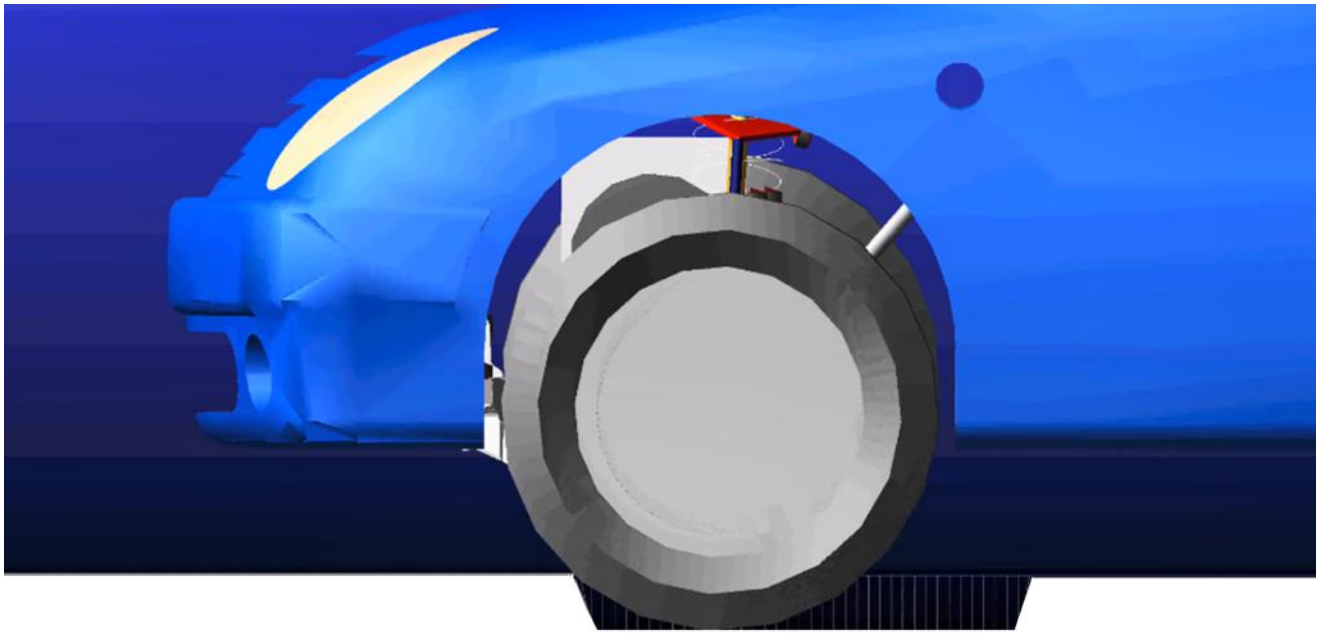

Converting dynamic impact events to equivalent static loads in vehicle chassis

Master's thesis in Applied Mechanics

Sushanth Shandliya Dattakumar
Vivek Ganeshan

Department of Applied Mechanics
CHALMERS UNIVERSITY OF TECHNOLOGY
Gothenburg, Sweden 2017

Master's thesis 2017:55

Converting dynamic impact events to equivalent static loads in vehicle chassis

Sushanth Shandliya Dattakumar
Vivek Ganeshan

CHALMERS
UNIVERSITY OF TECHNOLOGY

Department of Applied mechanics
Division of Division of Material and Computational Mechanics
Chalmers University of Technology
Gothenburg, Sweden 2017

Development of a method to convert dynamic impact events into equivalent static loads in vehicle chassis
SUSHANTH SHANDILYA DATTAKUMAR, VIVEK GANESHAN

Supervisor: Robert Hansson, ÅF Industry AB
Examiner: Prof. Ragnar Larsson, Chalmers University of technology

Master's Thesis 2017:55
ISSN number: 1652-8557
Department of Applied mechanics
Division of material and computational mechanics
Chalmers University of Technology
SE-412 96 Gothenburg
Telephone +46 31 772 1000

Cover: ADAMS simulation of the car front tyre being tested for the pothole drive in load case.

Chalmers Reproservice
Gothenburg, Sweden 2017

Converting dynamic impact events to equivalent static loads in vehicle chassis
Simulating the dynamic impact events in RADIOSS on vehicle chassis system to capture the peak load stresses and strains and replicating the event by applying equivalent static loads in optistruct
SUSHANTH SHANDILYA DATTAKUMAR
VIVEK GANESHAN
Department of Applied mechanics
Chalmers University of Technology

Abstract

The ever increasing need to simulate the complex dynamic events in vehicle chassis demands extensive computational resources. Due to the extreme nature of the peak load events, special attention needs to be given to the dynamic peak loads in order to understand the damage caused by them in the vehicle components and their effect on the design. To mitigate the difficulty of handling dynamic loads, structural engineers usually carry out the static simulations using a dynamic load factor. The dynamic load factors need to be reliable and determined logically by accounting for the inertial effects such that the equivalent static loads result in similar stress and strain patterns in the components.

The explicit method has been used extensively in order to effectively replicate the complex events due to its ability to solve highly non-linear problems with very less convergence issues and unconditional stability. However, the limiting factor being the computational time to carry out such analysis being very high. For quasi-static based problems, implicit methods have proven to be a good solution, as the computational time required in this method is shorter and the calculations cycles involved are fewer, but with an implication of conditional stability. Thus, its very important to understand the pros and cons of each integration scheme and choose the suitable one based on the application. In the current study, a methodology has been devised utilising both the schemes to arrive at a reliable dynamic load factor. The methodology involves carrying out the dynamic simulation first to replicate the dynamic event, followed by a modal transient analysis to understand the active modes at each time instant. The equivalent static loads are calculated based on the modal transient analysis and applied in static or quasi static analysis to obtain similar stress and strain patterns in the components and thus the dynamic load factor.

In the pre-study of the thesis, simple geometries such as the beams were tested for 2 configurations, namely, cantilever and simply supported. The physical and load impulse characteristics were investigated. In the main study, the project involved analysing the loading conditions from the multi-body dynamics model of the vehicle chassis components and developing an FE model to study the response of the sun-assembly to the applied dynamic and static loads. The equivalent static loads were adjusted to achieve the same damage (stress and strain distribution) in the components. The above procedure was adopted for 2 load cases, namely, the side kerb impact and the pothole load case. Parametric study was conducted to investi-

gate the effect of each parameter on the output response. The components studied in this work are the upper and the lower control arms of SLA type suspension system.

Some of the key findings from the thesis work are :

- Fundamental frequency of the sub-assembly governs the maximum displacement response.
- For the various load curves studied, namely triangular,sinusoidal, and trapezoidal pulse load, the maximum response was found to be mainly influenced by the average impulse acting on the system.
- The maximum displacement of the system is majorly governed by the ratio of the impulse duration to the fundamental time period of the system in case of isosceles triangular impulses.
- The dynamic peak load has negligible effect on the dynamic load factors.

Keywords: Impact events; Vehicle Chassis; Dynamic analysis; Equivalent static load.

Preface

The thesis was conducted for the partial fulfillment of the requirements of the MSc programme in Applied mechanics at Chalmers University of technology. The thesis work was carried out between Jan 2017 and June 2017 at ÅF Industry AB,Trollhättan. It was supervised by Robert Hansson from ÅF Industry AB and the examiner was Prof. Ragnar Larsson from the Department of Applied mechanics, Chalmers university of technology.

Acknowledgements

Firstly, we would like to thank Annika Aleryd, section Manager CAE & Safety for believing in us and giving us the opportunity to carry out our Master thesis work at ÅF Industry AB. Futhermore, we would like thank our supervisor Robert Hansson for his guidance, support and the encouraging environment he created for us to learn better. We would like to also thank our examiner Prof.Ragnar Larsson for being a great support system and helping us with valuable inputs in every meeting. A special thanks to all the support team from Altair with special mention of Fredrik Nordgren, Britta Käck and Joakim Truedsson for patiently helping us with all the software package related doubts and modelling. A special thanks to Gunnar Olsson for his valuable inputs during the intial phase and in the final presentation. Lastly, we would like to thank our parents for being great moral support throughout.

Sushanth Shandilya Dattakumar & Vivek Ganeshan, Gothenburg, June 2017

Contents

List of Figures

List of Tables

1
Introduction

1.1 Background

During its lifespan, vehicles are subjected to abusive/ impact loads several times, which are highly dynamic in nature. Such load cases are called as peak loads / strength events. Due to their extreme nature, simulating the peak load events with good accuracy is of great importance in the design and development cycle of various components in the vehicle chassis system. Some of the common scenarios of peak load events can be, driving over a curb stone, skid against a curb, driving into a pothole etc. [7]

Extensive research has been carried out focusing on the impact and fatigue analysis on the vehicle chassis system to identify the effects of these varying dynamic loads [2, 7, 15]. As it is computationally expensive to perform dynamic simulations , usually equivalent static loads are preferred to simulate the effect of such impact events. During dynamic analysis, special attention needs to be given to the peak loads due to the inertial effects. The applied static loads are multiplied with an amplification factor in order to accommodate for the inertia. The amplification factors used are usually obtained from experience, experimental and field data.

1.2 Purpose and Objectives

The thesis aims to study the dynamic impact events on vehicle chassis and to correlate this to an equivalent static load which results in a similar stress and strain distribution in the component. The aim of the project is to develop a method to identify a relation between the static and dynamic loads.

1.3 Method

A detailed literature study of the previous work pertaining to topics relevant to the thesis was carried out to understand the conversion of dynamic loads to static loads for simple geometries and reasonably complex geometries [8]. The dynamic simulation was initially carried out for simple geometries such as beams and equivalent static loads were obtained through optimisation using the package Hyperstudy and

also analytically.

The study was then extended to a system level analysis where 2 load cases were investigated, namely Pothole case and the side kerb impact case (Knuckle drop test) consisting of a few of the chassis components (namely lower and the upper control arms, the damper and the knuckle).The model setup is done using the preprocessor Hypermesh where the components are connected using bushings or ball joints. The dynamic simulation for the selected load case is performed using the explicit code RADIOSS after which a modal analysis is performed to identify the modes and to obtain modal participation of the identified modes at each time instant. The equivalent static loads are then obtained by activating the respective modes by tweaking the static loads. This is solved using the OPTISTRUCT, which has an in-built implicit code for quasi-static analysis. The loads are applied in static or quasi static simulations to obtain similar stress and strain distributions as observed in the dynamic simulations. Five different variations of the pothole load case with different damper configurations were tested and 1 case for the knuckle drop test case.

1.4 Limitations

- The thesis considers only the single impulse events such as a driving into a pothole or a lateral kerb strike. Thus, a fatigue analysis on the vehicle chassis will not be performed.
- Only short impulse events are considered for the study and quasi static events are not. Thus, the effects of prolonged load events that occur in situations like cornering or long distance braking are not considered for the study.
- The results obtained from the dynamic analysis will be used to develop a relation between the dynamic load acting on the vehicle and the applied equivalent static loads. Though they act as good indicators for design modifications, it is out of scope of the current research work.
- As the aim of the thesis is to obtain a correlation between the loads used in static and the dynamic simulation, there will be no physical validation of the obtained simulation results.

2

Theory

2.1 Static & dynamic study

Engineers often run into situations when they need to decide whether a static analysis would suffice their study or a dynamic one. To choose the right option, it is necessary to understand the complexity of the loading scenarios and the physics behind the study. In our case, we discuss further about the analysis of structures subjected to static and dynamic load cases and their differences.

Structural analysis deals with the change in behaviour of a physical member under the applied loads. The nature of response of the system is completely dependent on the way the load is applied to the component. If the load applied slowly, the inertial effect defined on the basis of Newton's first law of motion will be neglected and this is called as a static analysis. In static analysis, a single output value of solution is obtained for the system in the form of displacement, reaction forces etc. In a broader sense, static forces are considered as constant loads acting on the structure. A simple example of static load is a block of iron laying on a surface, a stationary truck etc.

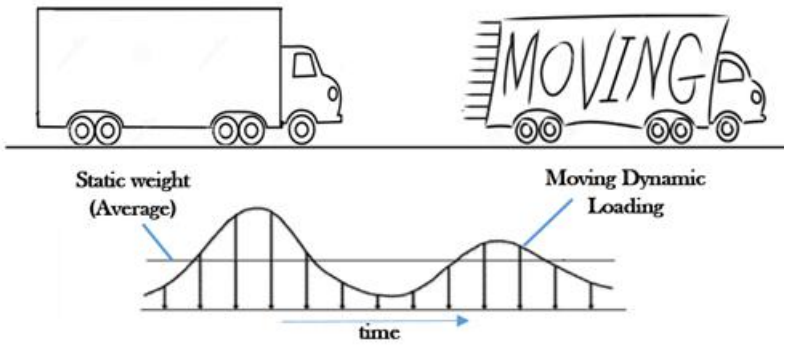

Figure 2.1: Representation of static and dynamic loads

Dynamic means time varying, and as the name suggests, the applied loads vary with time and thus induce time varying responses (displacements, velocities, accelerations, reaction forces, stresses etc). One of the most notable difference in dynamic analysis is the explicit consideration of inertial forces developed in the structure when it is excited by the time varying loads. Due to its time-varying characteristics, dynamic analysis is more realistic in nature to the actual occurring event but it also makes the modelling more computationally demanding. Some of the examples of

dynamic loads are hammer striking an iron block , a moving truck on a bridge etc. [12, 3]

2.2 Explicit & Implicit Methods

A model can be solved by either explicit or implicit numerical solution schemes. Implicit solvers are more suitable when the time dependency of the solution is not important (Eg. static problems,modal analysis) whereas explicit methods are suitable when solving for dynamic events. Depending on the type of analysis being performed a suitable solver method must be chosen such that the most accurate solution is obtained in the shortest duration and with more efficient resource consumption, as shown in fig 2.2. A discussion about the explicit and implicit method of solving a structural based problem is presented below.

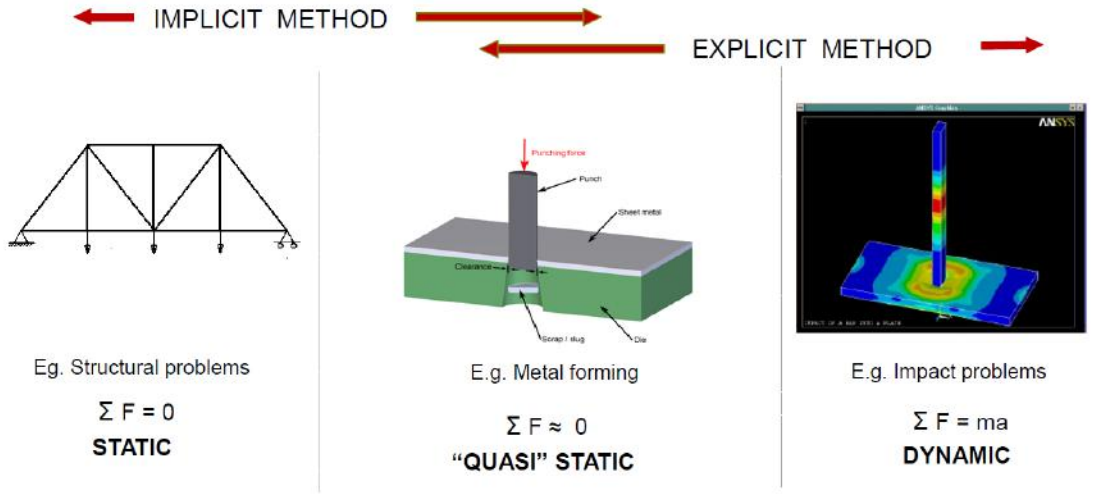

Figure 2.2: The figure represents the applicability of the implicit and the explicit methods

2.2.1 Explicit Scheme

The explicit scheme is used to solve dynamic problems. In this scheme, the state of the system is calculated at a later time step from the state of the system in the current time step. One of the common methods adopted to solve in this scheme is the second order accurate central difference method to approximate the accelerations in the body. The external forces are computed from the applied loading conditions. Then the internal forces due to stresses is computed using the implemented material model. Using the central difference scheme the acceleration is approximated as shown. The algorithm for the central difference scheme is as given.
The algorithm for the explicit method is shown below [5]

$$\ddot{u}_0 = \frac{p_0 - c\dot{u}_0 - ku_0}{m} \tag{2.1}$$

$$u_{-1} = u_0 - \Delta t \dot{u}_0 + \frac{\Delta t^2}{2} \ddot{u}_0 \tag{2.2}$$

$$\left[\frac{m}{\Delta t^2} + \frac{c}{2\Delta t}\right] u_{i+1} = p_i - \left[\frac{m}{\Delta t^2} - \frac{c}{2\Delta t}\right] u_{i-1} - \left[k - \frac{2m}{\Delta t^2}\right] \tag{2.3}$$

We can then calculate the displacement at the i+1 time step as

$$u_{i+1} = \frac{p_i - \left[\frac{m}{\Delta t^2} - \frac{c}{2\Delta t}\right] u_{i-1} - \left[k - \frac{2m}{\Delta t^2}\right]}{\left[\frac{m}{\Delta t^2} + \frac{c}{2\Delta t}\right]} \tag{2.4}$$

The velocity and acceleration are give by

$$\dot{u}_i = \frac{u_{i+1} - u_{i-1}}{2\Delta t} \quad \ddot{u}_i = \frac{u_{i+1} - 2u_i + u_{i-1}}{\Delta t^2} \tag{2.5}$$

To calculate the velocities and displacements of the consecutive time steps, i is replaced with i+1 in equations 2.4, 2.5.

From the incremental displacement the new internal forces and correspondingly the external forces can be calculated from loading conditions and the accelerations for the next time step can be computed [10, 5].

The explicit scheme is relatively inexpensive for high velocity and short duration events, as the mass matrix is inverted instead of the stiffness matrix(as in implicit scheme). The mass matrix being a diagonal matrix makes the numerical computation of its inverse quicker. The maximum time-step in an explicit solver is limited by the smallest element present in the model. For the solution to be stable, the enforced time-step for the analysis has to be smaller than the critical time step. The critical time-step is calculated using the following equation.

$$\Delta t = min_{elements}\left(\frac{l}{c}\right) \tag{2.6}$$

Time step should be chosen reasonably with reference to the above calculated value. As the time step is increased, the solver adds a non-physical mass to the system to accommodate for the time step. This affects the results of the dynamic analysis. Mass scaling is still acceptable when it does not affect the results considerably. Thus from the time-step formulation we observe that it depends on the speed of sound in the material (c) and the minimum element size (l) in the model.

2.2.2 Implicit Scheme

The implicit analysis enforces equilibrium between the external forces and the internal force using Newton or Newton-Raphson iteration method to a predefined tolerance. This allows it to be more accurate than the explicit analysis and larger

time-steps can be used to solve dynamic problems. At each time step the stiffness matrix needs to be updated, reconstructed and inverted which tends to be numerically expensive. Thus implicit analysis works best for static and quasi static cases where there are no dynamic or inertial effects and where the material plasticity needs to be captured.In the present thesis the implicit analysis is used instead of linear static analysis to obtain the obtain the mode transient analysis and also to calculate the equivalent static cases where significant plasticity was observed in the dynamic results.

One of the commonly used implicit methods is the Newmark method. Unlike the central difference scheme discussed previously which is conditionally stable, the Newmark method is unconditionally stable. The method computes the displacements and velocity for each time step using a Taylor series approximation. The algorithm for the Newmark method is given below.[5]

- The stiffness matrix $\mathbf{K}$, Mass matrix $\mathbf{M}$ and the damping matrix $\mathbf{C}$ are assembled.
- Initialise u_0, $\dot{u}_0$, $\ddot{u}_0$
- The timestep Δt and the parameters β and γ are chosen (for the solver to be unconditionally stable the parameters are chosen as follows $\gamma = 0.5$ and $\beta = 0.25$).
- The LU factorisation of the matrix given below is calculated

$$[\mathbf{M} + \gamma\mathbf{C} + \beta\Delta t^2\mathbf{K}] \tag{2.7}$$

- The initial displacement u_{-1} is computed as shown

$$u_{-1} = u_0 - \Delta t\dot{u}_0 + \frac{\Delta t^2}{2}\ddot{u}_0 \tag{2.8}$$

For each time step the displacement at time $t + \Delta t$ is calculated as

- The accelerations can be obtained by solving the equation given below

$$[\mathbf{M} + \gamma\mathbf{C} + \beta\Delta t^2\mathbf{K}]\ddot{u}_{n+1} = RHS \tag{2.9}$$

$$RHS = -\mathbf{K}u_n - (\mathbf{C} + \Delta t\mathbf{K})\dot{u}_n - \left[\Delta t(1-\gamma)\mathbf{C} + \frac{\Delta t^2}{2}(1-2\beta)\mathbf{K}\right]\ddot{u}_n \tag{2.10}$$

- The displacements and velocity can be computed as

$$u_{n+1} = u_n + \dot{u}_n\Delta t + [(1-2\beta)\ddot{u}_n + 2\beta\ddot{u}_{n+1}]\frac{\Delta t^2}{2} \tag{2.11}$$

$$\dot{u}_{n+1} = \dot{u}_n + [(1-\gamma)\ddot{u}_n + \gamma\ddot{u}_{n+1}]\Delta t \tag{2.12}$$

- The consecutive time steps are computed by updating n to n+1.

2.3 Linear & Non-Linear systems

In structural analysis, the systems can be modelled based on two main behaviours. One is accounting for only the linearity of the system and the other one accounting for both linearity and non-linearity. When a structure is loaded, it deforms. If the deformations are small or well below the elastic limit of the material, then the stiffness can be assumed to remain unchanged and the structure can be assumed to behave linearly. In the current study, the system experiences non-linear behaviour in terms of the plasticization of the components due to the applied loads and the peaking of stresses beyond the yield limit. The component displacement is governed by the bushing configurations at the joints, which exhibit a linear behaviour at lower displacements and a non-linear behaviour at large displacements, which is discussed in detail in section 4.1.4. The generic force-displacement relationship can be represented as follows,

$$F = kx \tag{2.13}$$

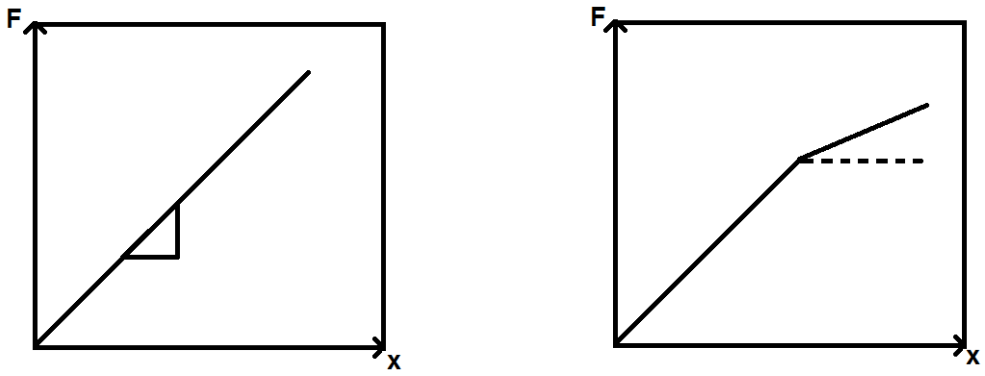

Figure 2.3: Material behaviour a) Elastic Response b) Elasto-plastic Response

This in turn implies that there will be no remarkable change in material properties and the shape of the structure. On the other hand, if the load applied results in a large or permanent deformation , then the stiffness of the system changes due to the plastic deformations and thus the material properties too. Such behaviour of the structure can be categorised as non-linear. The system can have other non linearity's such as the contact definitions and geometric non-linearity's. [16] .

Assuming perfect linearity in real structures is not an ideal way to go about in structural analysis because every system exhibits some degree of non-linearity in its response in the form of localised non-linearity's. Most of the problems can be solved with satisfactory accuracy by adopting proper linearization methods in the problem. But, the solution becomes unreliable if the degree of non-linearity in the system exceeds the capacity of the linear description. Non-linear systems can be solved to obtain reasonable solutions by using non-linear techniques such as iterative solution strategies [6].

2.4 Basic principles in dynamics

This chapter discusses the introduces the reader to the basic concepts in dynamics [1].

2.4.1 Work & Energy

An object in rest is said to be in static equilibrium when the net force acting on it zero. When a body in rest is disturbed by the application of an external force, it moves. By Newton's 2nd law of motion, acceleration of a body is directly proportional to the net force acting on the body and the mass of it. As the force increases, the acceleration of the body increases. Newton's 2nd law of motion is expressed as,

$$F = ma \tag{2.14}$$

When force (F) moves a body by a distance (S), then work is said to be performed on the body. The work-displacement relation ix expresses as,

$$W = FScos\theta \tag{2.15}$$

Where θ is angle between the direction of application of the force and the motion direction. Force is mostly variable in dynamic problems and hence it would be more apt to mention work as an integral over the position in space where force (F) is a function of position. The above can be expresses as,

$$W = \int_0^L F(x)dx \tag{2.16}$$

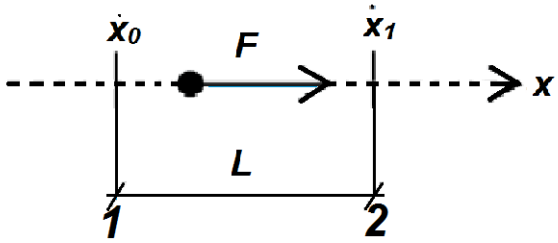

Figure 2.4: Work done on a particle

On integrating the equation of the Newtons 2nd law of of motion, the principle work-energy can be expressed as,

$$\sum W_{1-2} = \frac{1}{2}m{v_1}^2 - \frac{1}{2}m{v_0}^2 \tag{2.17}$$

$\sum W_{1-2}$ is the work done by the net forces acting on the particle to displace it from point 1 to 2. Work is a scalar quatity and it can be negative or positive.If the initial velocity (v_0) is not equal to the final velocity (v_1), there will be a change in kinetic energy in the system and this is equal to the work done by the force.

2.4.2 Momentum & Impulse

When bodies collide, they experience a variable force with respect to time acting on them during their interaction. This leads us to the principle of impulse and momentum. The time integral of the force, called as impulse is equal to product of mass and the change in velocity, known as the change in momentum. Consider a time interval t_1 to t_2 over which the force is integrated to obtain the following

$$\int_{t_1}^{t_2} F dt = m\Delta v \tag{2.18}$$

If a body moves with an initial velocity v_0,if a force F is subjected to it , the final velocity of the body can be calculated using the above equation. The impulse intensity can be determined by calculating the area under the force-time graph. An impact load is a force of large magnitude acting on a body for a very short duration, usually in the order of milliseconds. The physics behind impact loading involves the conservation of energy and momentum, i.e when a moving object collides with a structure it imparts its kinetic energy to the structure as an increase in strain energy and is partially dissipated through friction and plastic deformations in the structure and the object.

If the impact loading is a regular occurrence in the service of a structure, then it is expected that the plastic deformation occurring in the structure during impact loading is localized and the overall response of the structure is elastic after the impact load. One of the most common example is the drop impact test shown in figure 3. This is usually done by dropping a known mass from a predetermined height onto a structure like a beam. If the resulting response of the structure is purely elastic, then a relationship can be established between the static and dynamic loadings of the dropped mass as shown

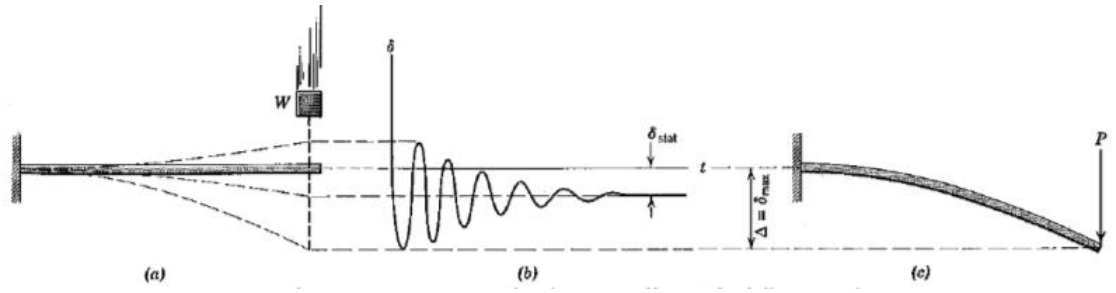

Figure 2.5: Mass impact test for beams

$$n = 1 + \sqrt{1 + \frac{2h}{\delta_{static}}} \tag{2.19}$$

The above formulation is a simplified version of the dynamic impact factor and does not take into account modal vibrations. A more detailed analysis which accounts for the modal vibrations will be presented later. [1]

2.4.3 Structural dynamics and solving methods

A typical structural dynamics problem can be defined based on the d'Alembert's principle. FEM being one of the common discretization method adopted to solve the problem by breaking up the continuous system into smaller finite parts, the equation of motion can be defined based on mass (M), damping (C) and stiffness (K) as follows [11] :

$$M\ddot{x} + C\dot{x} + Kx = F(t) \tag{2.20}$$

where, $\ddot{x}$,$\dot{x}$ and x are the vectors of nodal acceleration, velocity and displacement respectively. F(t) is the applied external load. The system is said to be in dynamical equilibrium if the above equation is satisfied at all times, t.[11]
Structural dynamic problems can be classified as shown in Fig 2.6 based on the nature of the external load and the expected outcome of the problem.

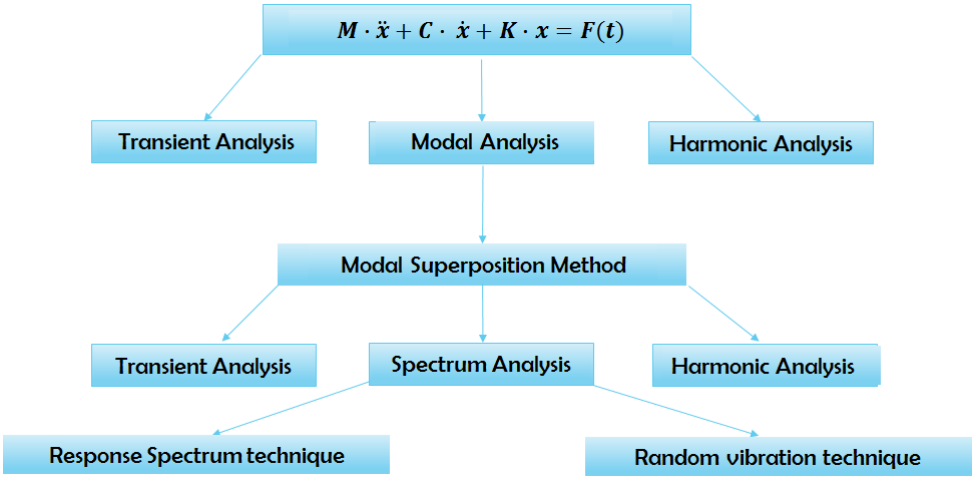

Figure 2.6: Classification of structural dynamics problems

Among the various methods mentioned, modal analysis and transient analysis are discussed in detail, as it is of special importance in this study.

2.4.3.1 Modal analysis

Modal analysis is used to understand the vibration characteristics of the system. It enables the designer in understanding the mode shapes for the natural frequencies of the system. The rhs in the eqn. 2.24 is considered zero in modal analysis. [11] Modal superposition method can be used quite effectively to study the dynamic response of the system based on the modal analysis. Modal analysis is a linear analysis and thus any non-linearity's mentioned will be ignored.

2.4.3.2 Modal superposition method

Mode superposition method is one of the efficient ways to replicate a harmonic or transient analysis [11]. In this method, the dynamic behaviour of the system

is obtained by the linear combination of the first m prominent modes.It can be represented as,

$$x(t) = \sum_{n=1}^{m} \phi_n.y(t) \tag{2.21}$$

Where ϕ_n represents the mode shape of mode n and y(t) is its modal amplitude. On substituting eqn. 2.21 in eqn. 2.24 and by pre-mulitplying with the transpose of the modal matrix , we arrive at the following equation:

$$\phi^T M\phi.\ddot{y}(t) + \phi^T C\phi.\dot{y}(t) + \phi^T K.y(t) = \phi^T.F(t) \tag{2.22}$$

For an undamped or symmetrically damped system, the above equation represents a set of m equations which describe the generalised SDOF model in modal subspace [11].

2.4.3.3 Transient Dynamic analysis

Transient dynamic analysis is the method adopted to determine the dynamic response of a system to a time varying load acting on it. The time-varying load is mentioned as a vector in the RHS of eqn. 2.24 . The analysis can be used to determine the stress, displacement, strain and reaction force time histories of a system for combination of harmonic or transient loads. For determining the solutions in this method, time integration should be performed . As discussed in section 2.2 , either explicit or implicit solving algorithm can be can be adopted.

2.5 Single degree of freedom systems

A single degree system is one in which the motion of the body is defined by a single coordinate. Fig 2.7 represents a similar spring-mass-damper system acted upon by a time-varying force (F) [1]. This body is considered to be rigid and has no internal deformations when loaded. In an reality, systems exhibit some damping properties due to the frictional forces created internally and due to the contact with the ground, due to which the system is modelled along with a damper for more realistic behaviour. The equation of motion can be can be written as,

$$m\ddot{x} + c\dot{x} + kx = F(t) \tag{2.23}$$

The equation of motion can be solved to calculate the variation of displacement with time by substituing for the loading function, initial conditions and other necessary parameters.
An SDOF system can experience a free vibration or forced-vibrations based on the force acting on the system. When a system is subjected to impact loading, the force acts on the body for a short interval of time. The systems response can be explained in two parts, namely, the response during the load application and the free vibration response after the removal of the load. As the load duration is typically short, the maximum response of the system occurs slightly later [8]. The characteristic of the response depends on the type of the load and also the property of the structure

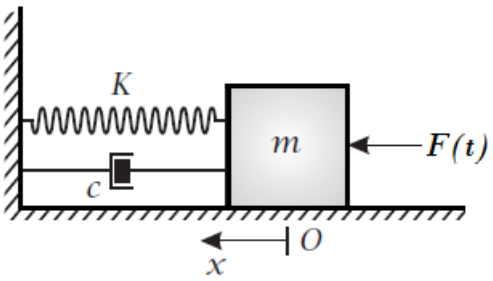

Figure 2.7: SDOF spring-mass-damper system

[1]. The effect of damping is negligible for the first oscillation but become of more prominence in the consequent ones. Thus, it would not be of necessity to include dampers for capturing the maximum responses of the impact loaded systems. [8]

2.6 Optimization and sampling techniques

In the most general sense, optimization is the mathematical discipline adopted to find the extreme(maxima and minima) of systems, functions or set of numbers. The prime motive of all the optimization techniques is to either maximize the desirable outcome of a system or minimize the undesirable outcomes. A system comprises of inputs, design variables, controllable and uncontrollable factors. The output of this system is the response.As the number of variables in a system increases, understanding the interaction and influece of them on the response of the system gets challenging. Sampling techniques are the methods adopted to decide the number of samples to be chosen in the design space to extract maximum information using minimum resources.

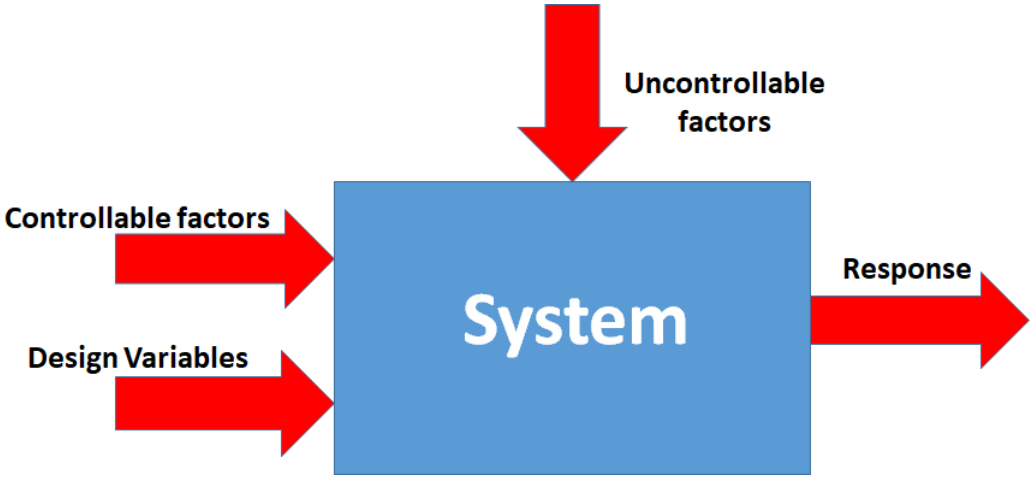

Figure 2.8: System setup

The following section discusses one of the standard sampling techniques, design of experiments and an optimization technique using global response surface method in detail.

2.6.1 Design of experiments

DOE is one of the mathematical methods used to plan and perform scientific studies systematically. DOE enables one in understanding the effect of multiple input variables on the response of the system. It can be adopted in finding the optimal settings of the input variables to obtain a specific response of the system. Some of the common techniques in DOE are full factorial method, fractional factorial method, Taguchi method etc. Among the methods mentioned, Taguchi method has been adopted in this work and is discussed in detail in this section.

- **Taguchi method**

Taguchi technique is a method used to find the best values of the controllable factors such that there is very less sensitivity to the uncontrollable factors. It helps in carefully choosing the samples from the full factorial set so that the main effects of the input variables can be captured in the response of the system. The method uses a special method called as the orthogonal arrays for sampling. The orthogonal array and its size depends on the number of input variables and levels of each variables chosen.

$$N_{taguchi} = 1 + \sum_{n=1}^{m} (L_n - 1) \tag{2.24}$$

Where 'm' is the no. of variables and 'L' is the no. of levels.

2.6.2 Load Identification

Load identification is the process of finding equivalent static loads for and applied dynamic loads. One of the methodology explored was load identification via system identification. The system identification uses optimisation to fit a set of output response of a model to predefined target values by varying the input variables.The objective function for the system identification is formulated using the least squares formula [14]. The optimisation was then carried out using the Global Response Surface Method (GRSM) to identify the equivalent static loads.

2.6.3 Global Response Surface Method

The optimisation technique used in the system identification is the Global Response Surface Method.As the name suggest its a method which is used when a global optimum is required. During each iteration of the GRSM new designs are generated. The response surface is then updated adaptively in accordance with newly generated designs. The figure below gives the simplified algorithm of the GRSM[14].

2.7 Suspension systems

The suspension system is one of the most important component in the vehicle. It has to keep the vehicle in contact with road surface while at the same time preventing vibrations, shocks due to bumps or potholes to be transmitted to the vehicle body. ,thus ensuring a good ride performance and comfort for the passengers in the vehicle.

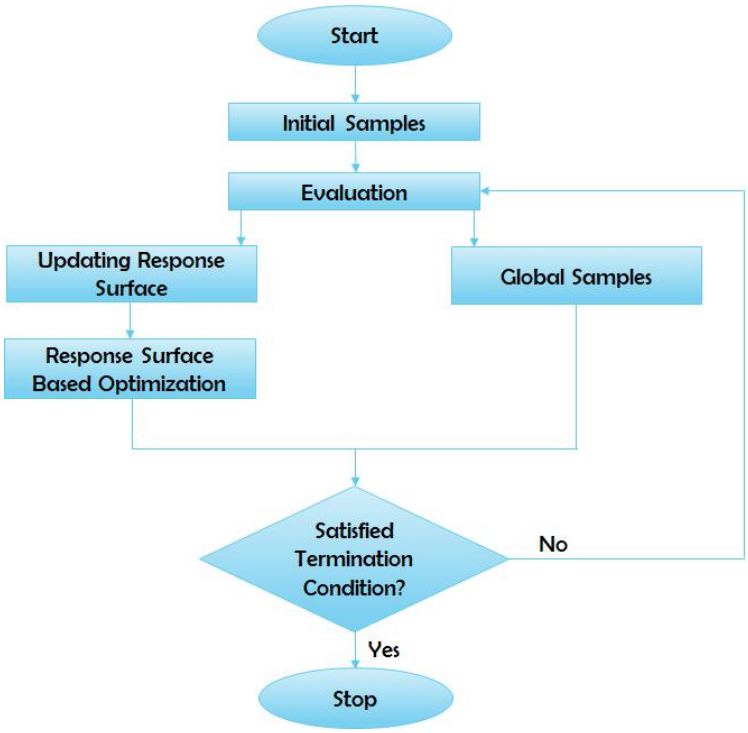

Figure 2.9: GRSM Algorithm

The scope of the current thesis is limited to only the double wishbones suspension system and different load cases are studied for the same suspension system.

2.7.1 Suspension System

The double wishbone suspension system is an independent suspensions system.The wheels can move independent of each other. Thus, a disturbance in one wheel will not be transmitted to the other wheel. It consists of two wishbone shaped link arms whose one end is connected to the knuckle by means of spherical joints and the other end to the chassis via two mounting points. In this study we use a variant of the double wishbone suspension system is the Short Long Arm (SLA) suspension system.The lower control arms support the vehicle load and the upper arm helps in maintaining the position of the steering knuckle. The suspension damper configurations usually used in the such systems are telescopic type. The spring stiffness and the damping properties of the suspension system can be tweaked to adjust the ride quality and the performance of the vehicle.[4, 15]

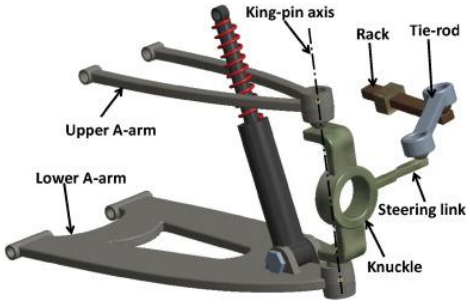

Figure 2.10: Double Wishbone Suspension System [15]

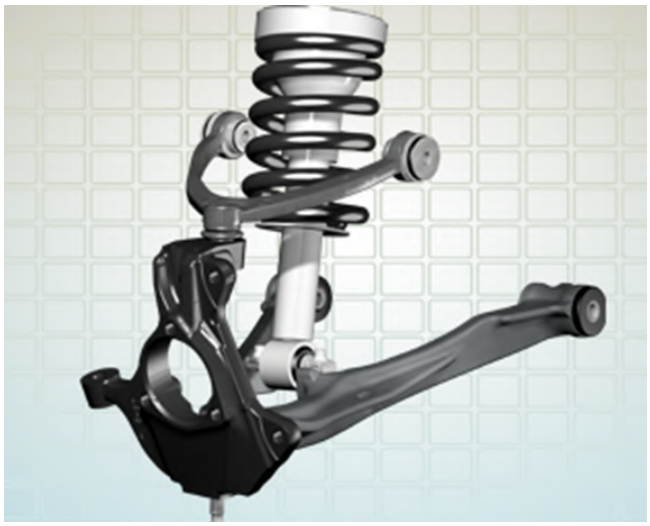

Figure 2.11: Short Long Arm (SLA) type suspension system

3

Pre-study on Cantilever and simply-supported beams

3.1 Continuous formulation of beams

Continuous formulation is often an ideal method for studying the behaviour of mechanical structures, as infinite number of degrees of freedom are defined in the system i.e each small element can be considered as a discrete particle which is connected to all other elements by springs.In this method, the mass is assumed to be distributed equally throughout the structure rather than being concentrated at localised coordinates, as in lumped parameter based models. [1].

3.1.1 Static solution

The static solution for the beam problem was obtained by implementing the Euler-Bernoulli beam theory from which a relation between the distributed force (q) and the transverse beam deflection (y) can be established as shown in eqn 3.1.

$$\frac{q}{EI} = \frac{d^4y}{dx^4} \tag{3.1}$$

Where E $\rightarrow$ Young's modulus
I $\rightarrow$ second moment of inertia
q $\rightarrow$ load per unit length

To determine the static deflection of the beam, the differential equation in eqn. 3.1 is integrated 4 successive times and solved with appropriate boundary conditions to get the transverse deflections. The appropriate boundary conditions for different configurations of beams is available in various literature's [1, 9]. Some of the approximations considered while implementing Euler–Bernoulli beam theory are:-
(1) shear deformations are ignored,and
(2) planar cross sections remain normal and planar to the axis of the beam during deformation. The accuracy of the model are limited by these assumptions when the beam is not long and slender.

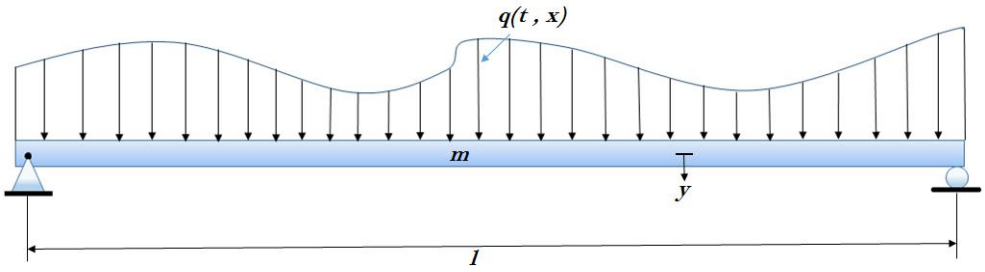

Figure 3.1: Beam with distributed mass and load

3.1.2 Dynamic solution

To determine the analytical solution for the dynamic response of the system, Lagrange's equations were used[1]. Concentrated load was applied at the mid span and end point for the simply supported and the cantilever beam respectively.The following steps were followed to arrive at the analytical solution :
The dynamic deflection of the continuous beam can be represented as the summation of its modal components as shown in the equation below i.e mode super-positioning.

$$y(t,x) = \sum_{1}^{n} A_n(t)\phi_n(x) \tag{3.2}$$

A_n is the modal amplitude, ϕ_n is the characteristic shape. The equation of motion of the nth mode can be obtained by solving the given differential equation.

$$\ddot{A}_n + \omega_n^2 A_n = \frac{f(t)\int_0^l p_1(x)\phi_n(x)\,dx}{m\int_0^l \phi_n^2(x)\,dx} \tag{3.3}$$

Thus the static modal displacement is computed and corresponding dynamic modal amplitude is obtained as shown

$$A_{net} = \frac{f(t)\int_0^l p_1(x)\phi_n(x)\,dx}{m\omega_n^2\int_0^l \phi_n^2(x)\,dx} \tag{3.4}$$

The modal responses are given by,

$$A_n(t) = A_{net}(DLF)_n \tag{3.5}$$

Where $(DLF)_n \rightarrow$ dynamic load factor for equivalent SDOF system in nth mode (refer fig.2.8 in [1])

The total response of the system can be calculated as,

$$y(x,t) = \sum^{n} A_n(t)\phi_n(x) \tag{3.6}$$

Where $\phi_n(x) \rightarrow$ Characteristic shape for beams with various boundary conditions (refer Table.4.1 in [1])

3.2 Response of the beam to different pulse-load characteristics

Response of the beam was studied for Three different pulse-load characteristics, namely triangular,sinusoidal, and trapezoidal pulse load as shown in Fig.3.2. Impulse load of 20ms and 4ms were imposed on a cantilever beam for all the three loading curves. As seen in Fig 3.3, the peak deflection in case of beam loaded the trapezoidal pulse load was the highest followed by sinusoidal pulse and triangular pulse load respectively.This is evident from the fact the area under the load curves shown in Fig. 3.2 is highest for the trapezoidal loading indicating that it has the maximum impulse amongst the loading's that were tested for. Also, the peak event occurs at a slightly later time period in case for the trapezoidal loaded beam in comparison to the triangular pulse loaded beam. These characteristic responses can be attributed to the higher impulse acting on the beam in case of trapezoidal loading.

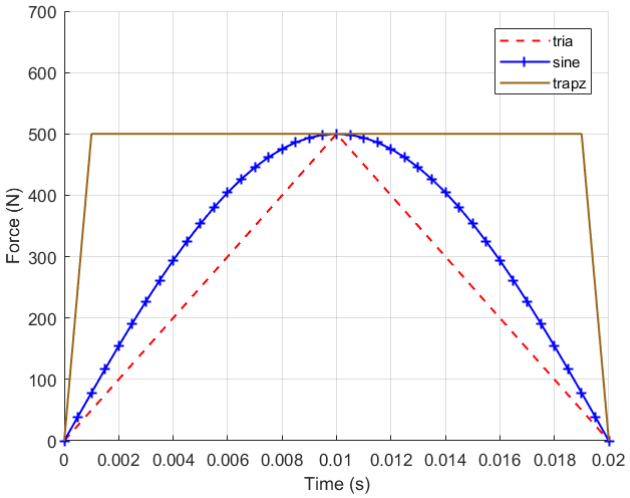

Figure 3.2: Impulse Load curve

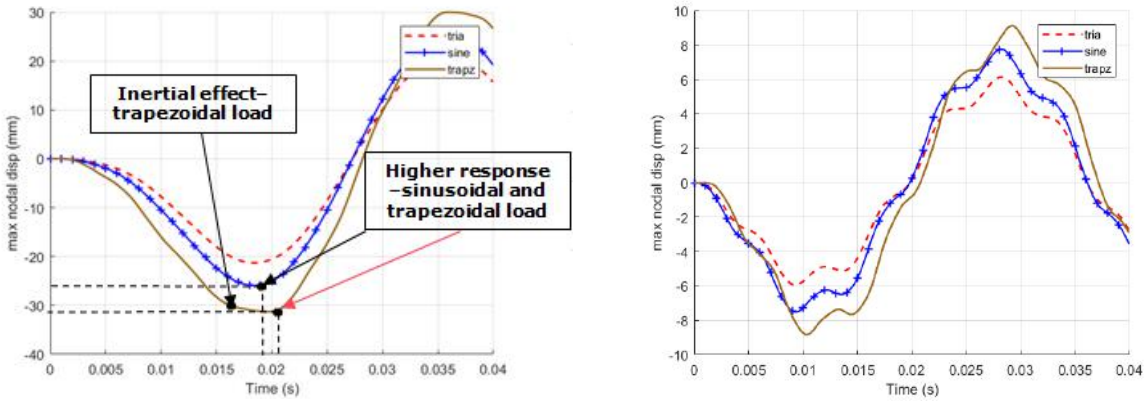

Figure 3.3: Maximum nodal displacement of cantilever beam (500x100x10) for different loading curves acting for a)20 ms b)4ms

3.3 Load Identification Setup

Load identification was carried out to compare and match the dynamic response of the beam to its equivalent static model, which would give a similar displacement and stress fields at a particular time instant. The dynamic simulations of the beams were setup in Hypermesh and solved using the explicit FEM solver RADIOSS. Triangular impulse loads (as shown in Fig 3.2) were applied on two beam configurations, namely cantilever and simply supported beam. The dynamic simulation was run for few milliseconds till at-least one cycle of the response was captured. Nodal displacement were captured on several points along the length of the beam in order to conduct a load identification based optimisation on the geometry using the software package Hyperstudy. The equivalent static model to match the obtained dynamic displacements in the RADIOSS was setup in Optistruct and the forces were applied at the points of interest along the length of the beam as shown in Fig 3.4 .

The Optistruct model was then imported into Hyperstudy. The static forces on

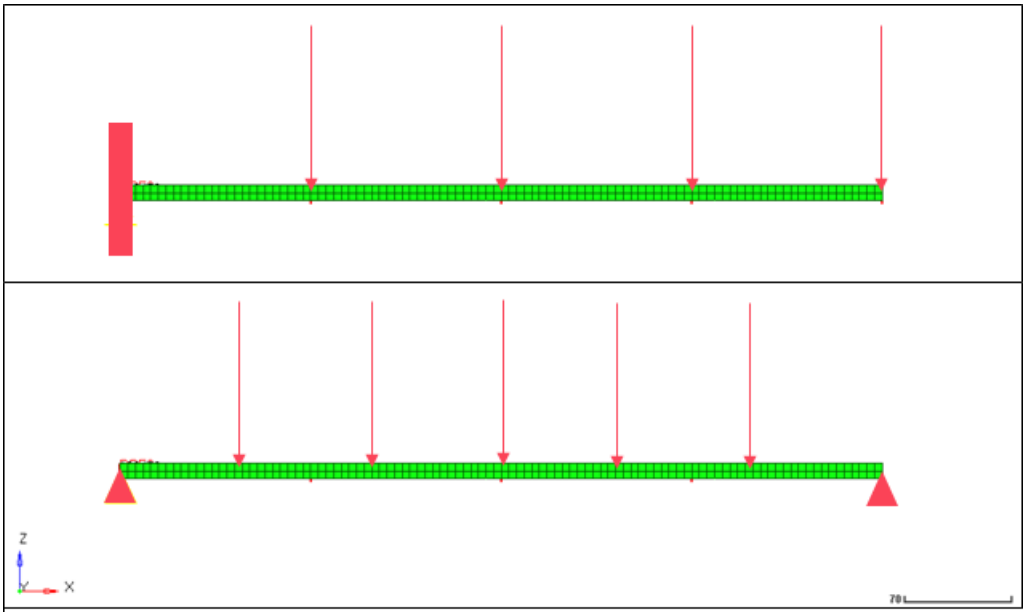

Figure 3.4: Load-identification model setup in Optistruct with points picked along the length of the beam

the points of interest (Fig 3.4) were set as the design variables and the nodal displacements/stresses from the dynamic simulations at the point of interests were set as the target responses. System identification was performed using the Global Response Surface Method (GRSM) to determine the equivalent static forces at the nodes picked. Also, the system identification method was tested on the system to study the stress responses and found to yield good results.

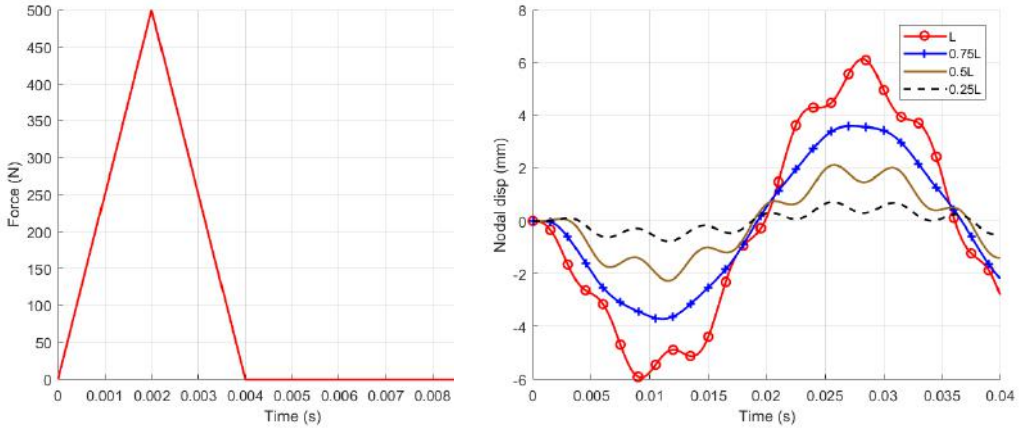

Figure 3.5: a) Impulse load acting on a cantilever beam (500x100x10) b)The corresponding nodal displacements at various points along length beam

3.4 Pre-Study Results

The transient response of the beam subjected to an impulse load was studied. Tables in appendix I aggregate the results obtained from load identification for the displacement and the stress distribution for simple beam problems. Impulse loading duration ranging from 4 ms up to 24 ms were imposed on the beams of different cross-sections and 2 different configurations to capture the displacement and stress responses. It was observed that the shorter impulses in the range of 1/5th to 1/10th the fundamental time period of the system, caused the beams to vibrate in one of its modes, primarily in the 1st mode followed by some minor contributions from the 2nd and the 3rd mode (as indicated in Fig. 3.9 for cantilever beam and Fig 3.13 for simply supported beam), this is confirmed by looking at the mode participation factors obtained from performing the modal transient analysis as seen in Fig 3.10. As the impulse duration was shortened, the contributions from the higher modes become more pronounced [1, 9, 2]. As the duration of the impulse was increased, the maximum displacement in the beam increased but the inertial effect was reduced (i.e the peak event occurred more closer to the peak load timing in the impulse) due to the fact that the rate of loading was reduced [1]. The Dynamic load factors (DLF) were calculated based on the results obtained and it was found to vary from 0.5 upto 20. One noticeably different result is the value of DLF being lower than 1 in case 3 in simply-supported beam (Table A.2). This is due to the impulse duration being nearly 1/4th the natural time period of the beam. In triangular impulse loads, the dynamic effect increases as the duration of loading approaches the natural period of the system and reaches the maximum when it is equal to it [1]. Fig 3.6 shows the parameter based study carried out to study the response of the system for triangular impulse loads. The DLF is observed to be sensitive to the time period of loading. As the mass of the system was increased, the amount of energy required to displace the beam from rest will be more. The mass increase resulted in smaller displacements as compared to the lighter beams, thus resulting in the drop of DLF value with increasing mass. The peak value of the force has no effect on the DLF

due to the fact that DLF is relative in nature to the static displacements. The time to reach the peak loads would be more important than the peak values of the force. It was evident from this study that the DLF and response of a system subjected to an impact load not only depends on the system parameters like mass, stiffness and damping, but also on the characteristics of the load like, duration of the impulse, rate of loading and also the point of application of the load. The calculated analytical dynamic displacements were in close convergence with the RADIOSS response with an error percentage of 7 - 9 %.

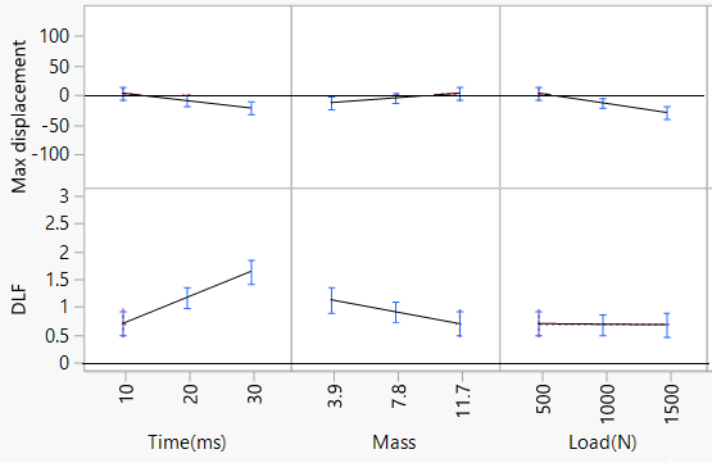

Figure 3.6: Parameter based study of the cantilever beam for isosceles triangular load

The equivalent static loads obtained from the system identification were applied on the static model of the beam. The nodal displacements and element stresses along the beam length were recorded, as shown in the table A.2. The displacements and stresses due to the applied equivalent static loads matched well with the results obtained from the dynamic simulations. The comparison of the displacement and stress field in the dynamic and equivalent static, as seen in figures 3.7 and 3.8, show a close correspondence between the dynamic and equivalent static simulations.

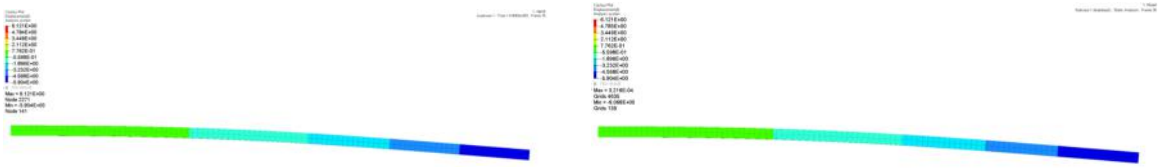

Figure 3.7: Displacement contour plots for a)Dynamic (4ms 500N impluse) and b) Equivalent static loads acting on a cantilever beam

3.5 Key findings

Some of the key findings from the pre-study are :

- Fundamental frequency of the beams govern the maximum displacement response of the system
- For the various load curves studied, namely triangular,sinusoidal, and trapezoidal pulse load, the maximum response was found to be mainly influenced by the average impulse on acting on the beam
- The maximum displacement of the system is majorly governed by the ratio of the impulse duration to the fundamental time period of the system in case of isosceles triangular impulse
- System identification using hyperstudy and the modal transient analysis was found to compliment each other in order to identify the equivalent static load case in case of simple geometries like beams, as shown in fig.3.7 - 3.14.
- The dynamic peak load has negligible effect on the dynamic load factors as shown in fig 3.6.

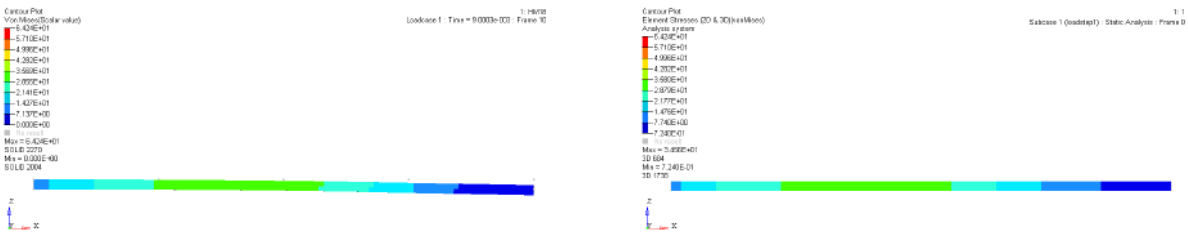

Figure 3.8: Stress contour plots for a)Dynamic (4ms 500N impluse) and b) Equivalent static loads acting on a cantilever beam

Figure 3.9: Eigen modes of the cantilever beam a) Mode 1 b) Mode 2 c) Mode 3

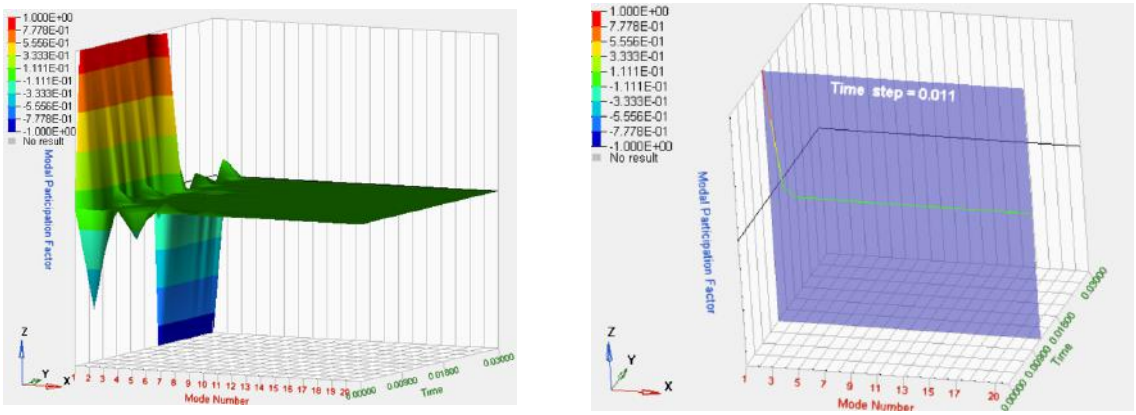

Figure 3.10: Modal transient analysis of beams with the active modes (1 & 2) at peak instant

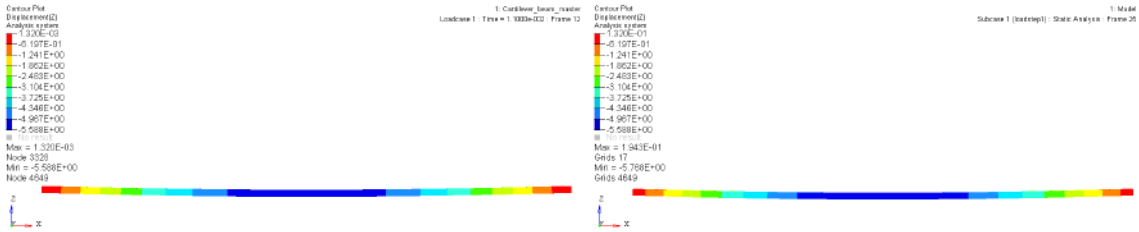

Figure 3.11: a) Dynamic and b) Equivalent static displacement response comparison of simply supported beam under the influence of dynamic (1000N 8ms) impulse

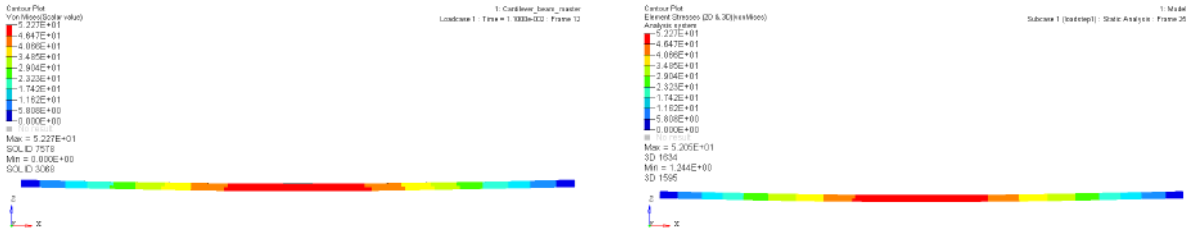

Figure 3.12: a) Dynamic and b) Equivalent static stress response comparison of simply supported beam under the influence of dynamic (750N 4ms) impulse

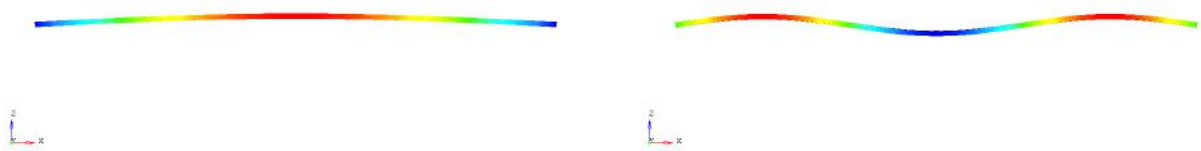

Figure 3.13: Eigen Modes of simply supported beam a)Mode 1 and b)Mode 3

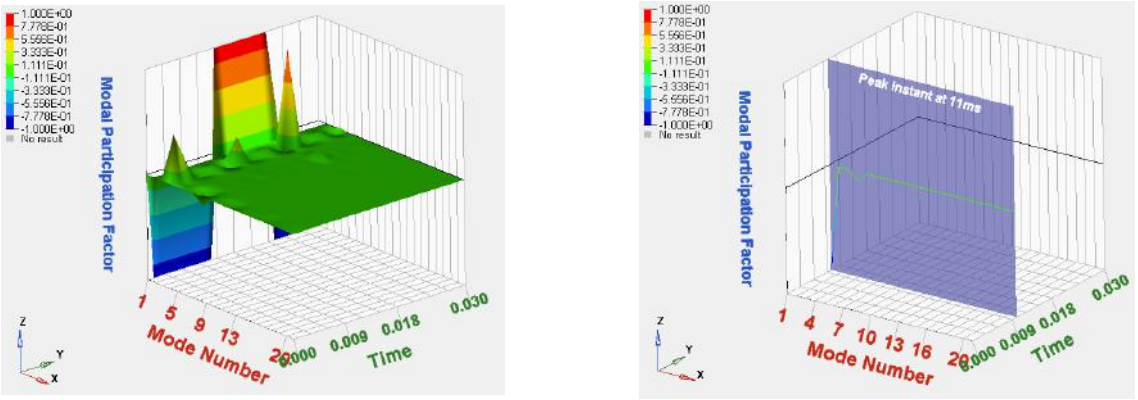

Figure 3.14: Modal transient analysis of simply supported beam showing a) modes active b) modes active at peak instant

4

Model Setup

4.1 Dynamic Model Setup

The dynamic simulation was setup in the explicit finite element code RADIOSS. The setup of the model required certain approximations and simplifications, so that the model predicts sufficiently accurate results at a reasonable time while replicating the physical behaviour of the suspension system for the given purpose. The details of the setup are discussed in detail below.

4.1.1 Model setup & Description

The vehicle assembly under study was setup previously for an NVH based study . Considering the system setup and the boundary conditions were the same for the purpose of the current study, the Nastran model was utilised to understand and setup the dynamic analysis for the front suspension assembly. Hypermesh had a built in conversion tool that enabled us to convert the Nastran model into a radioss model. As the front suspension included many components which would increase the complexity of the problem, a quarter vehicle model consisting of the wheel hub, knuckle,shock absorber, upper and lower control arms was considered.The Nastran model was converted into a RADIOSS model for the study purpose. The ball joints in the assembly were modelled using RBE2 elements. RBE2 spiders were created at the joint locations for each of the components, which were in turn connected by a single RBE2 element. In order to replicate a ball joint, the only the translational DOFs were locked in the RBE2 spiders and the connector single RBE2 element, thus giving it a free movement in all the 3 rotational DOFs, as represented in Fig 4.1. A global contact definition (Type 24) was defined for the assembly to ensure that the local interaction between the components is captured. The inner ends of the link arms were constrained with an single point constraint (SPC) through the bushing elements (SPRING 3N) which allows the link arms to move, as they would in a vehicle. The damper system was defined using the beam elements (BEAM 3N) connected to lower ball joint on one end and to the spring element (SPRING 2N with a local fixed coordinate system) near the upper strut. Figure 4.1 represents the overview of the assembly setup with details about the SPC's.
In order to obtain reasonable results, the time step should be sufficiently small to avoid mass scaling issues. Based on the size of the elements and the suggestion by Hypermesh, the time step was set to 6 x 10^{-8}.

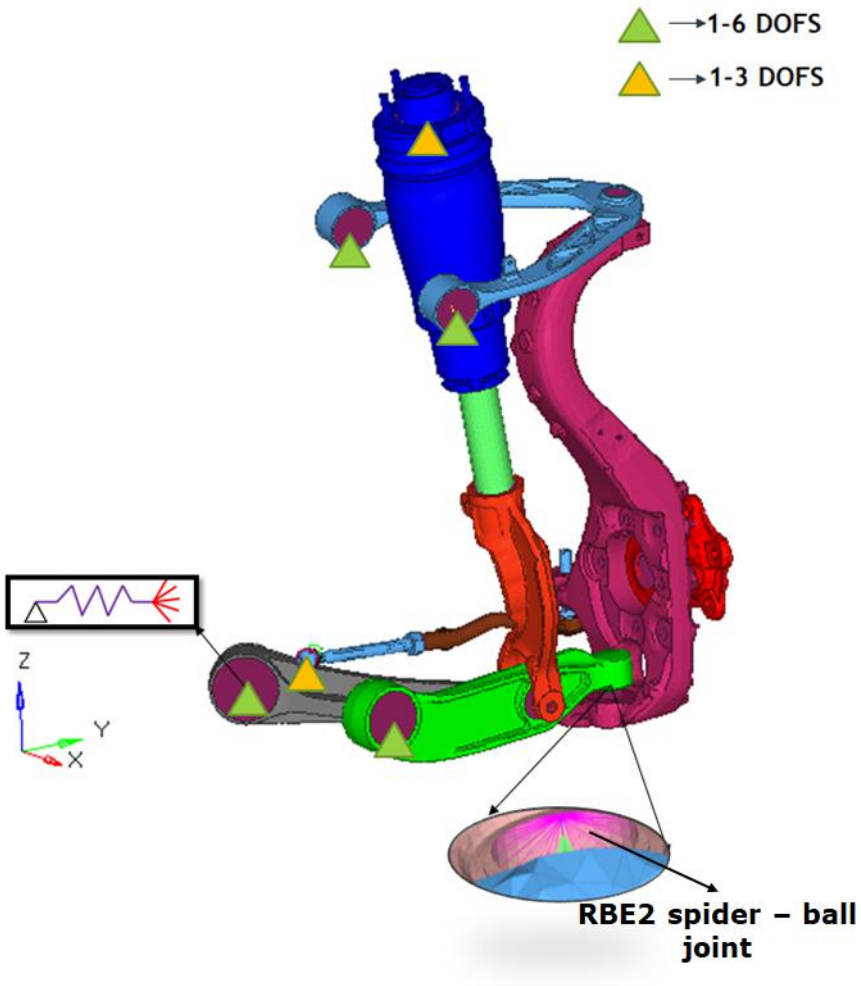

Figure 4.1: Model setup of the sub-assembly used in the current study

4.1.2 Load application

The points load were applied through the Force-time load curves at the hard points through the master node of the RBE2 spiders. The load curves were obtained from the ADAMS simulations for each of the load cases. The load cases tested in this work are lateral kerb impact and drive through a pothole. The load cases are discussed in detail below:

- **Knuckle drop test - Lateral Kerb impact**

In this case, a lateral point load was applied through the RBE2 elements at the test setup plate end as shown in fig 4.2.

- **Drive into a pothole**

In this case, a point load was applied in each of the global directions through the master node of the RBE2 spider as shown in the fig 4.3.

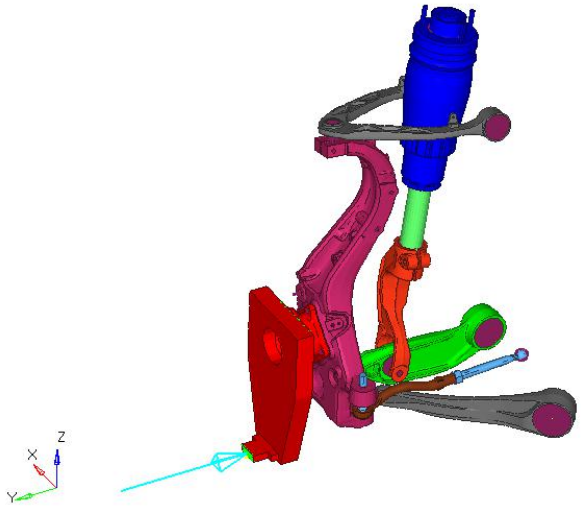

Figure 4.2: Model setup - Knuckle drop test -Lateral Kerb impact.The blue arrow shows the direction of the lateral kerb load. The attachment plate is included to in place of the wheel, as per the knuckle drop test setup, as shown in the picture alongside

4.1.3 Material model

The material model is one of the most important parameter for any simulation. It defines how the material will respond to the applied loading and when it will start yielding. RADIOSS has the option to either use a predefined material model from its library or to have a user defined material model by specifying the load deflection curve. In the present thesis, the Johnson Cook material model was chosen from the RADIOSS material model Library.

The Johnson cook model is an empirical model which takes into consideration isotropic hardening, kinematic hardening,temperature effects and variation of yield stress of the material.The stress in the Johnson Cook model is given as follows [13].

$$\sigma = (A + B \cdot \epsilon_p^n)\left(1 + C \cdot ln\frac{\dot{\epsilon}}{\dot{\epsilon}_0}\right)\left(1 - \left(\frac{T - T_r}{T_m - T_r}\right)^m\right) \tag{4.1}$$

Where ϵ_p is the plastic strain, T_m melting point,T_r room temperature and A,B,C,n,m,ϵ_0 the material parameters.In the current study we will not be considering strain rate or temperature effects on the material, hence the material parameters which are required are A,B and n. From experimental data its easy to obtain the yield stress (A), ultimate stress(σ_u) and strain(ϵ_u) from which the values of B and n can be calculated using the following equations [14]

$$A = \sigma_y \tag{4.2}$$

$$n = \frac{\sigma_u \epsilon_u}{\sigma_u - \sigma_y} \tag{4.3}$$

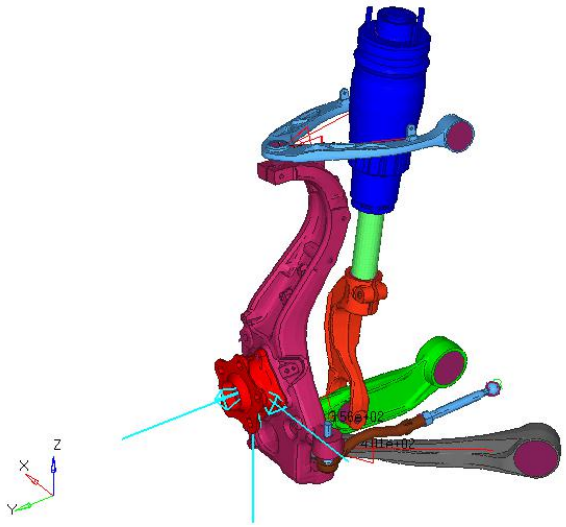

Figure 4.3: Model setup - Pothole load case. The 3 blue arrows at the hub represents the loads in the 3 directions for the load case

$$B = \frac{\sigma_u}{n\epsilon_u^{n-1}} \tag{4.4}$$

The constants C and T_m can be ignored as the strain rate effects and temperatures effects are not considered in this study, in order to simplify the model.

4.1.4 Bushing Modelling

The lower and the upper control arm is connected to the sub-frame through the bushings. The bushings play an important role in the behaviour of the system.The dynamic characteristics of the bushings are complex in nature, as the response depends on variables such as frequency, preload, amplitude etc.[15]. The static stiffness (force-displacement) curves had to be modelled to obtain a reasonable solution. The non-linear bushings were modelled based on the inner and outer diameter of the bushings housing. The asymptotes were included for the curves keeping the outer diameter of the bushing housing as the maximum displacement for the bushings. A modelled bushing with an asymptotic behaviour included as discussed above, is shown in figure 4.4.

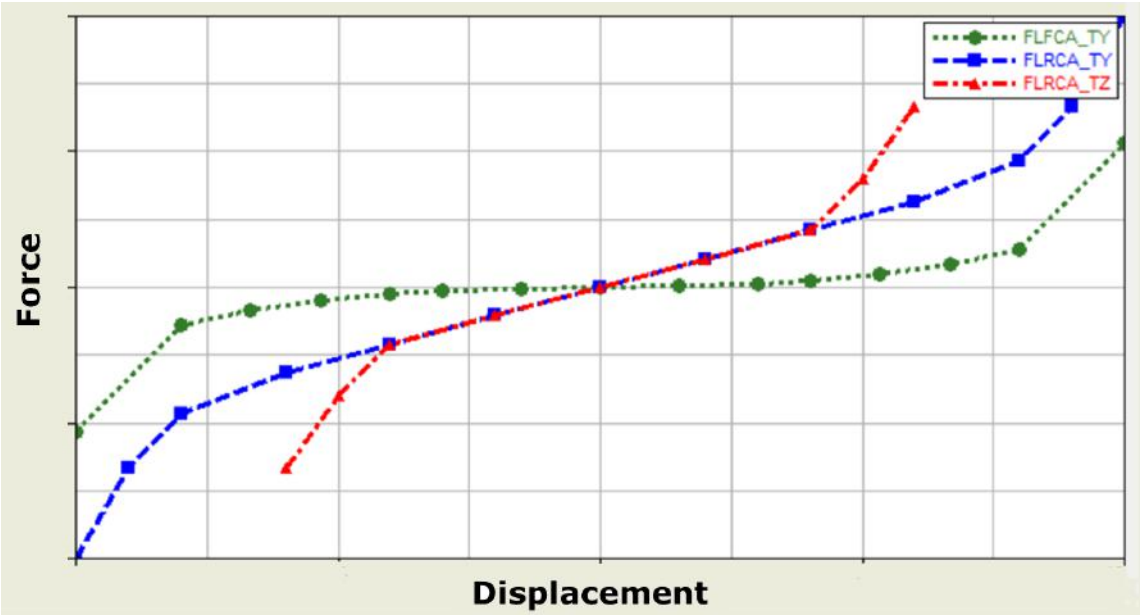

Figure 4.4: Force vs. Displacement curves of the modelled bushings with asymptotes at the outer diameter of the bushings for few of the translational directions for FLRCA and FLFCA

4.2 Linear static, Quasi Static and Modal Transient Analysis Model Setup

The linear static, non-linear quasi static and modal transient simulation were solved using the FEM solver, Optistruct. Modal transient analysis is a dynamic simulation based on mode superposition method with linear material properties defined.

4.2.1 Model Setup

For all the above simulations, the NVH (Noise Vibration and Harshness) model which was setup in NASTRAN was used as the starting point. The components were modelled keeping the dynamic model setup as a reference so that simulations could be compared. There was no contact defined in these models in order to reduce the simulation run-time.The absence of a contact definition would allow the tie rod to rotate about its axis in a rigid body mode.To prevent the rigid body motion of the tie-rod (in rotation) a local coordinate system was define along the length of the tie-rod and the axial rotation of the tie rod was constrained.

4.2.2 Load Application

In linear static and the quasi static models, the loads were applied as point loads at the wheel hub in the pothole case and at the adapter end for the knuckle drop test, as discussed in the dynamic model setup. In case of the modal transient analysis,

the loads were applied as point loads through the constraints (DAREA) with a force vs. time table(TABLED1) defined for the time varying load.

4.2.3 Material Model

In case of the modal and quasi static analysis the material models chosen were different. The modal and static analysis are always performed using the linear elastic isotropic material properties. This is one of the major limiting factors in the modal analysis as it does not account for any material non linearity, but its observed that this assumption is good enough to achieve the desired output as seen in the results section.
The quasi static analysis was performed to capture the plasticity which occurs in the component during loading. Using the user defined material model option MATS1 in Optistruct a bi-linear load curve as seen in Fig.2.3 is defined using the yield stress,ultimate stress and strain of the material.

4.2.4 Bushing Modelling

The bushings modelled for the dynamic simulations were used.

5
Methodology and Load cases

5.1 Method

Based on the pre-study and literature survey, a methodology was developed to arrive at the equivalent static loads. Figure 5.1 shows the procedure, which worked well for the load cases tested in the present thesis.

The procedure is described in detail in steps below:

- **Step 1 :** The non-linear dynamic analysis is carried out to understand the behaviour of the system. The displacements at the hard points in x,y and z directions are recorded for the required time instant (peak instant in the current study). The stress distributions and plastic strain in the components are noted.
- **Step 2 :** An eigen mode analysis is carried out to understand the global and local eigen modes in the sub-assembly under study.
- **Step 3 :** A modal transient analysis is carried out to replicate the dynamic analysis and to understand the active modes in the system at each time instant of the analysis.
- **Step 4 :** The Modal participation factor and the effective modal mass was used as reference points to understand the contributions and the percentage of mass participating in each mode. This step helps in understanding the complexity of the scenario being tested based on the number and the type of modes active in the system.
- **Step 5 :** Unit loads are applied in the global x,y & z directions individually on the static assembly setup to record the displacements in each direction.
- **Step 6 :** The loads are scaled in the individual directions to match the displacement fields recorded in step 1 at the hard points, keeping track of the stress fields in the components. It can be noted that the maximum scaling directions are supported by the mode participation factors and the effective modal mass.
- **Step 7 :** If the stress and the strain distributions are reasonably mapped, the equivalent static loads are obtained or we move to step 8.
- **Step 8 :** A more detailed load identification needs to be carried out, which can be:
  (i) Hard point based load identification, where loads need to be added at specific hard points to activate the similar modes, as in dynamic analysis in the system

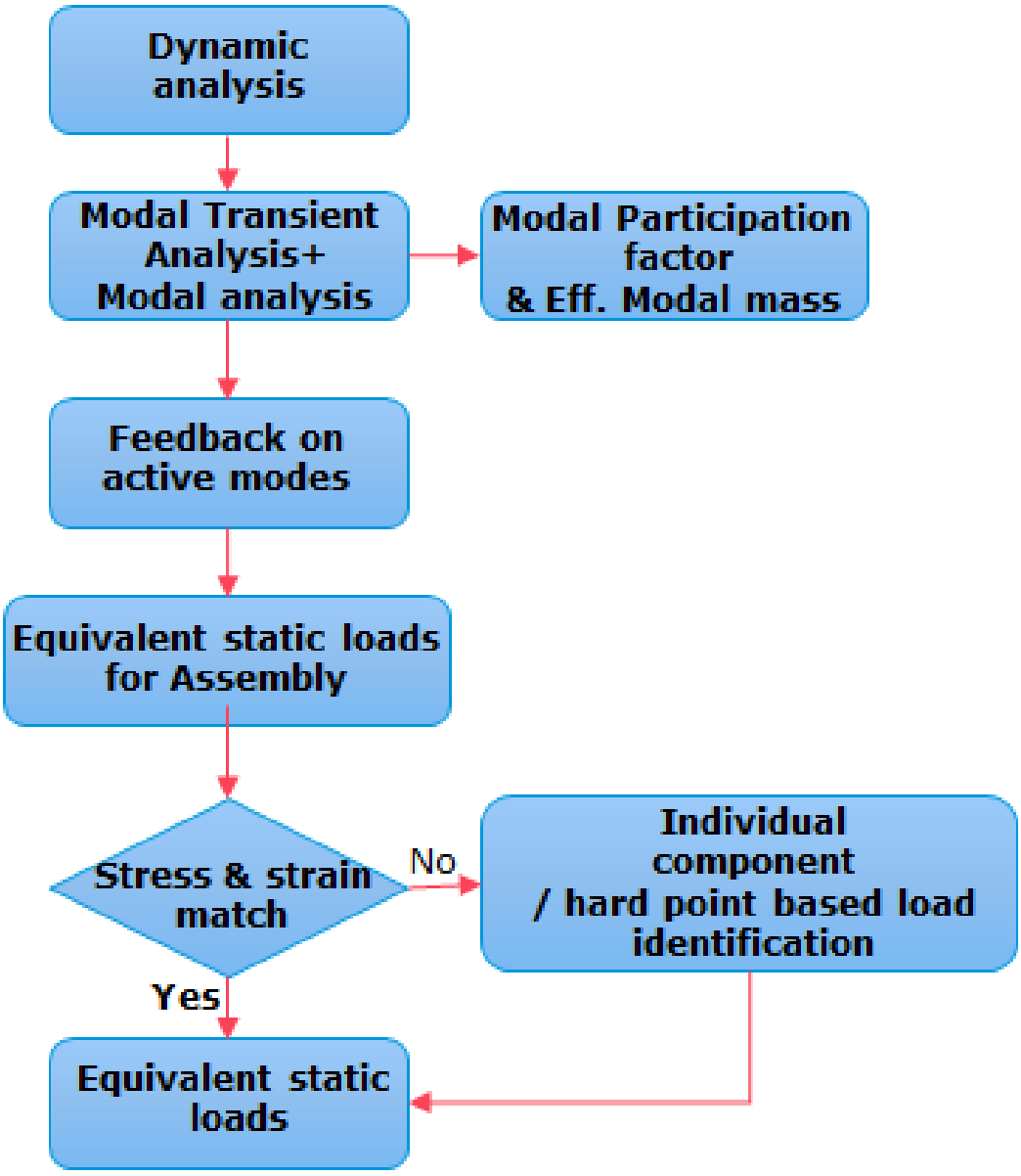

Figure 5.1: Flow Chart - Methodology

(ii) Component based load identification, where the components will need to be analysed individually to understand the loads acting at its hard points This step has not been considered in detail in this study.

Note: As the number of mode interactions in the system gets higher, it becomes more challenging to obtain. Specially, when the local modes are active, it becomes more challenging to capture the dynamic stress and plastic strains in the components.

Pothole load cases		
No.	Damper	Velocity (kmph)
1	Inter	35
2	Soft	40
3	Soft	35
4	Stiff	50
5	Inter	22
Kerb impact load case		
No.	Impact Mass (kg)	Velocity (m/s)
1	700	2.2

Table 5.1: Load cases

5.2 Load cases

As discussed in the previous chapter, two load cases were mainly tested in this thesis.

- **Pothole load case**

The pothole load case was tested for various velocities of the car and damper configurations as shown in Table 5.5 and Fig 5.3. 3 configurations of dampers, namely stiff, intermediate and soft damper. Fig5.3(a) shows the maximum tire normal force for different velocities and damper configurations simulated in ADAMS.

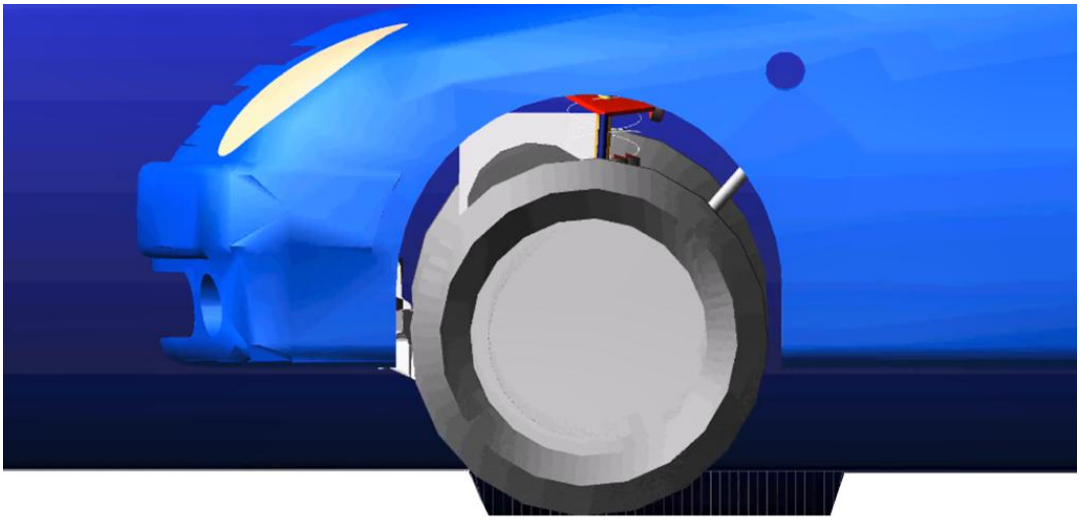

Figure 5.2: Adams simulation of the pothole load case

Figure 5.3: a) Max tire normal force vs velocity b) Damper curves

- **Kerb impact case - Knuckle drop test**

Table 5.5 shows the input parameters for the knuckle drop test, which is a industry standardized test to analyze side kerb impact in vehicle chassis.

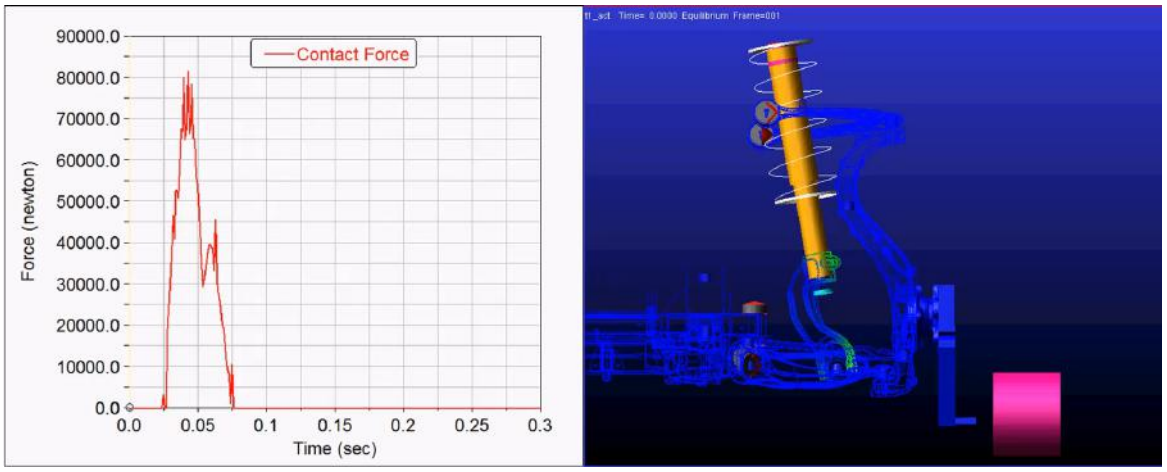

Figure 5.4: Adams simulation of the side kerb impact load case

5.3 Load curves

The input load curves for each of the cases mentioned in the previous section were obtained through the ADAMS multi-body simulations. As the load curves were noisy, specially in case of the kerb impact case, the curves were smoothened in MATLAB using the Gaussian function, as shown in fig 5.5.

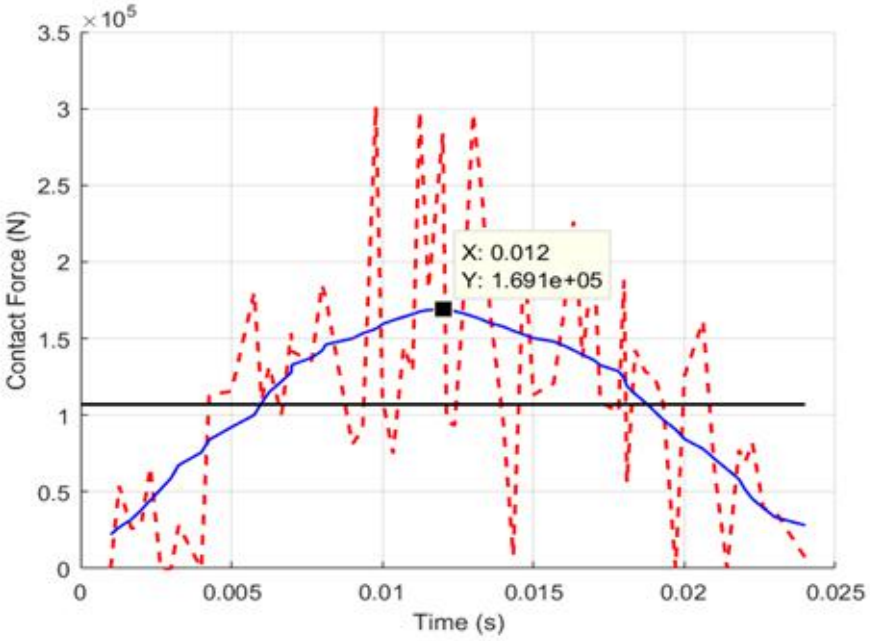

Figure 5.5: Smoothened ADAMS load curve for the side kerb impact load case

6
Results

The chapter discusses the results obtained by adopting the methodology discussed in the previous chapter.

6.1 Pothole load case

The system was tested for 5 different load cases as shown in Table 5.5 . The equivalent static loads were calculated for the peak instant from the dynamic simulation in all cases. Load case 1 is discussed in detail. The modal transient analysis suggested that mode 3 (global mode, z-translational) and mode 4 (x-translational) had participation of 1 and 0.3 respectively at the peak instant of 41ms in the dynamic simulation as shown in fig 6.1. These values were kept as reference values to understand the contribution of each modes to the total response of the system at the peak time instant, which suggests that the maximum scaling direction to be z-translational in this load case. Unit displacements were applied in x,y and z directions individually on the static model setup to understand the displacement fields of the system. Based on the observations, the dynamic peak loads had to be scaled by a factor of 1.11 in x- direction and by 1.56 in the z-direction at the wheel hub to obtain the equivalent static loads. The scaling of loads were carried out keeping the von-mises stress and the displacement fields as the reference points. Fig6.4 compares the stress distribution in the most affected part in this load case, which was the rear lower control arm.As seen, the applied equivalent static loads replicate the stress pattern in the components well. The stress values in the other components showed good correlation to the dynamic results too.

Table 6.1 shows the results for all the tested load cases. It can be noted that the scaling factor varies from 1.27-1.58 for the z-direction loads.The scaling factor was observed to depend on the loading duration and the nature of the load curve. If the time duration of the load from crest to crest is larger, the scaling factor was found to be higher for these cases, which can be attributed to higher net impulse in these cases. Biggs (1964) has explained the scaling factors for SDOF systems, where the duration of loads are compared with the fundamental time period of the system. If we approximate the load curves to an isosceles triangular impulse, the scaling factor increases as the duration approaches the fundamental time period of the system. More rate based and time duration of loading based studies were done, which is discussed in the following section.

Case Descr.	Direction	Dynamic Peak loads (N)	Eq. Static loads (N)	Scaling factor	Comments
1 (35kmph, Inter damper)	X	8376	9600	1.11	**Minor contributions – X-trans mode** **Most affected mode – Z-trans**
	Z	27133.7	**42500 (6g)**	**1.56**	
2 (40kmph, Soft damper)	X	12908.4	13600	1.1	
	Z	45624.1	**57200 (9g)**	**1.27**	
3 (35kmph, Soft damper)	X	13593.9	14600	1.1	
	Z	34412.2	**46200 (7g)**	**1.34**	
4 (50kmph, Stiff damper)	X	3141.69	3500	1.11	
	Z	18038.5	**28500 (4g)**	**1.58**	
5 (22kmph, Inter damper)	X	2506	2700	1.1	
	Z	15264.2	**24200 (3g)**	**1.58**	

Table 6.1: Results- Pothole load cases

6.2 Knuckle drop test - Kerb Impact case

Apart from the pothole load case, the system was also tested for a kerb impact event where a mass of 700 kg travelling at 2.2 m/s impacts the assembly shown in Fig. 4.2. The equivalent load was calculated at the instant when the peak stress occurred in the most affected component (rear control arm in this case). The stresses peaked at 27ms in the components when the bushings went into non-linearity. The modal transient analysis suggested that there were significant contributions from multiple modes unlike the pothole case where only two global modes predominantly contributed to the response of the system. From figure 6.5 it can be observed that there were significant contributions from mode 3 (z-translation of knuckle, global mode), 8 (knuckle rotation about the z-axis) and 11 (knuckle rotation about x-axis) with a mode participation of 0.6,-1 and 0.5 respectively. Some minor contribution is observed from many other modes such as mode 6,7, 9(local mode), 13 and 17. As multiple modes are active at the peak instant it becomes quite challenging to capture all the modes by scaling just the Y direction force in the static solution. Thus in this load case more significance is given to capture the stress and strain hot spots on the most affected components (front lower rear control arm) in this case. A load in y-direction caused the knuckle to move in y-translation and rotate about the z-axis. As mode 8 gives us good judgement that the z-rotation of the knuckle is a dominant mode, the y-direction forces had to be scaled the most followed by mode 11 which suggests that the knuckle had to rotate about the x-axis .
The y direction force had to be scaled by a factor of 1.33 and an additional force of 15KN was to be applied in z direction to reasonably capture the stress distribution

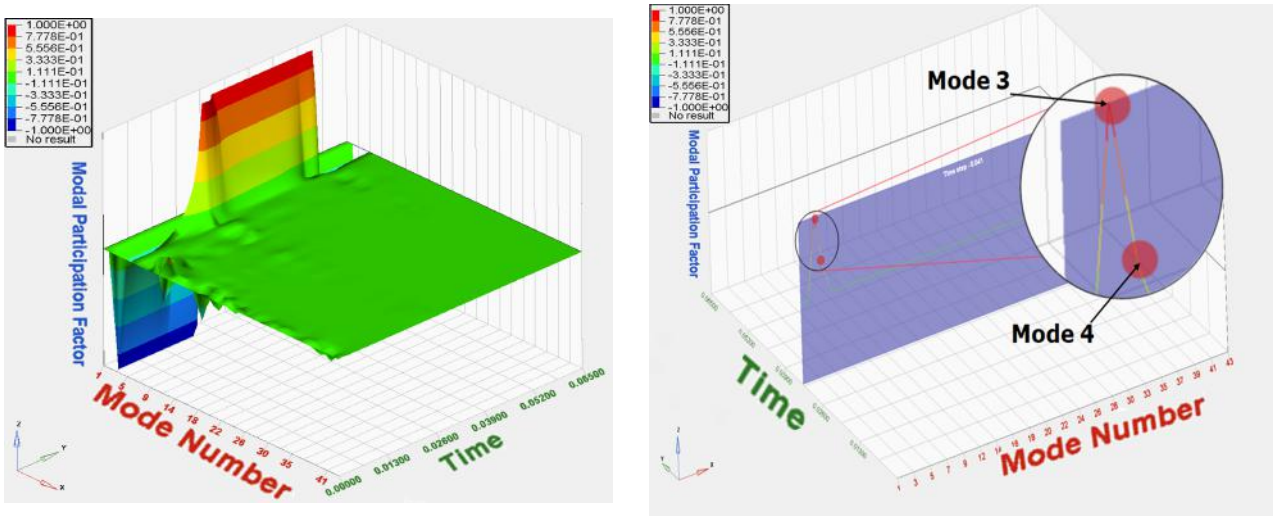

Figure 6.1: a) Modal transient analysis for the Pothole load case 1 b) Active modes at the peak instant at 41ms

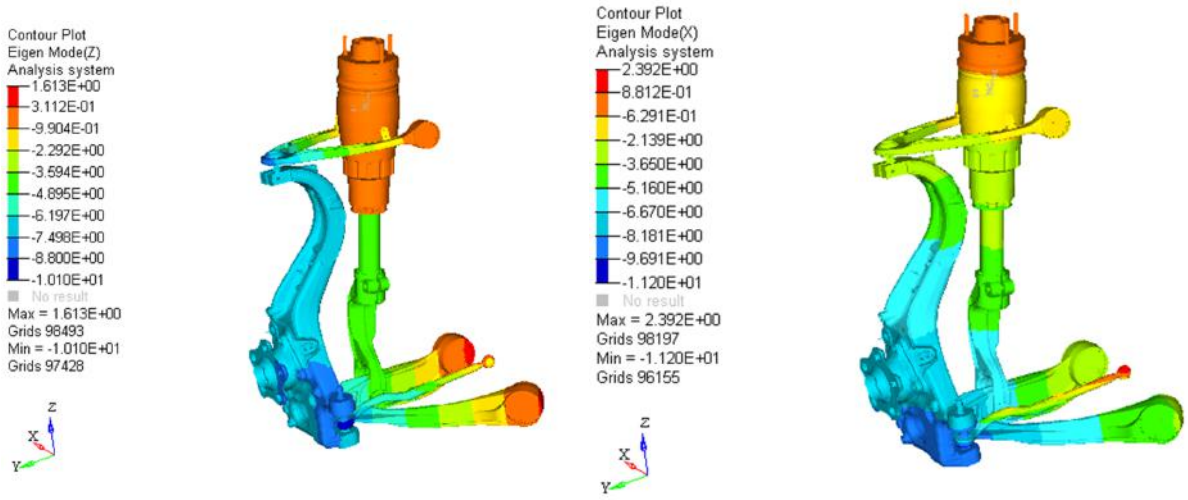

Figure 6.2: a) Mode 3 - Knuckle z-translation b) Mode 4 - Knuckle x-translation

in the components as shown in Table 6.2. From Fig 6.7 and 6.8 it can be seen that even though the stress and plastic strain distribution in the dynamic and equivalent static simulation are not mapped exactly, the equivalent static solution was able to capture the hot spots in the component well. Ideally, as the local mode interactions increase in the dynamic simulation, a reasonable orientation of the solution would be to capture the most affected zones in the components rather than the exact stress and strain distributions, as the stress in the bodies are path dependant.

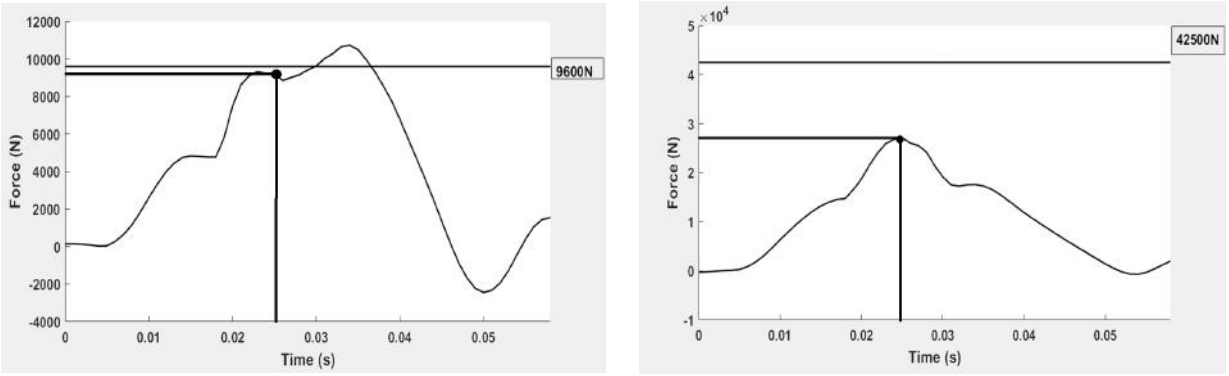

Figure 6.3: Equivalent static loads in x and z-directions compared with the load curves - Load case 1

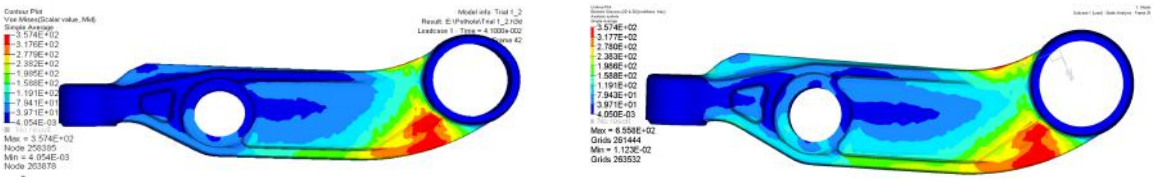

Figure 6.4: Von-mises stress comparison for lower rear control arm - Pothole case

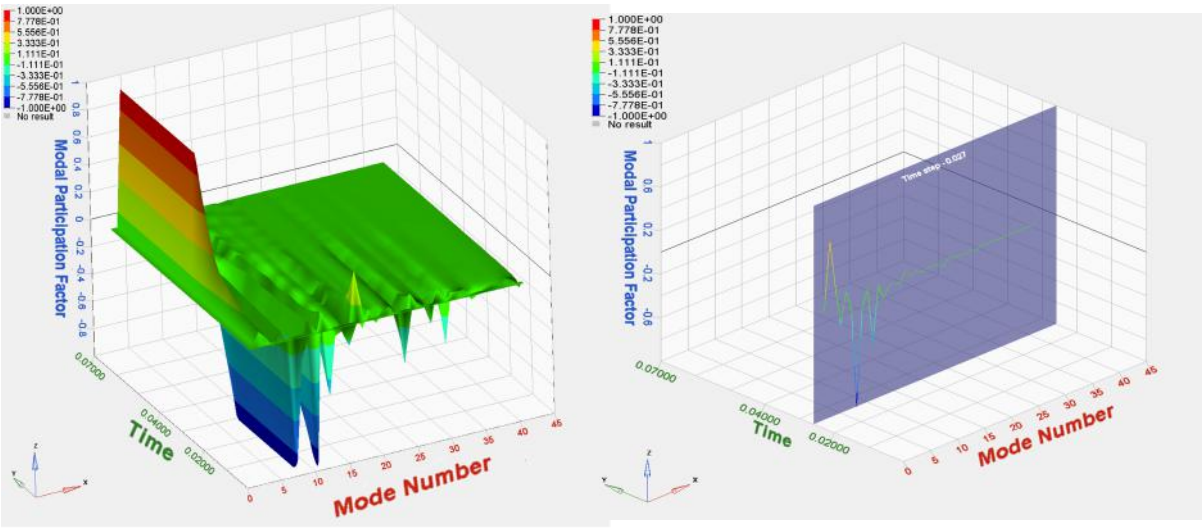

Figure 6.5: a) Modal transient analysis - Kerb impact case b) Active modes in the system at the time, 27ms

Load Case	Direction	Dynamic Peak loads (N)	Eq. Static loads (N)	Scaling factor
1 (Kerb Impact 2.2 m/s)	Y	80398	105000 (8g)	1.30
	Z	--	15000	--

Table 6.2: Results - Lateral kerb impact load cases

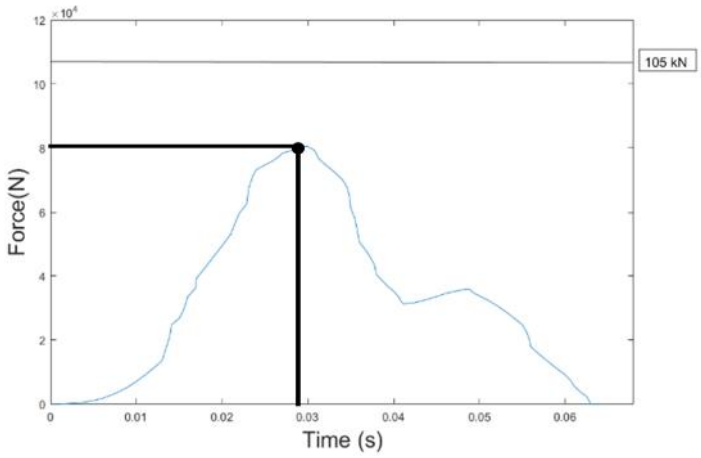

Figure 6.6: Equivalent static loads in y-direction compared with the load curves

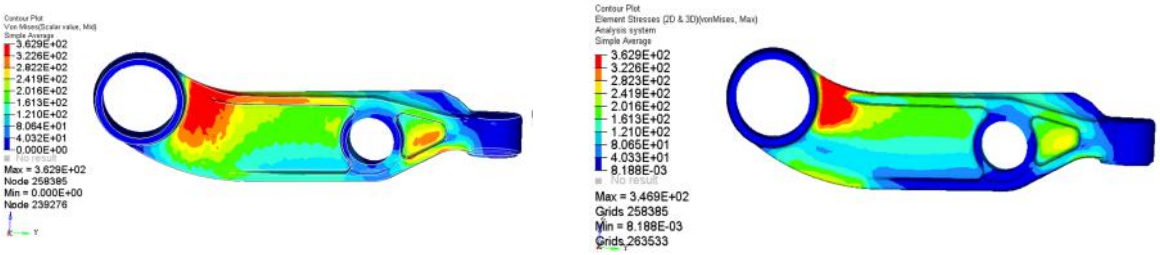

Figure 6.7: Stress distribution - Kerb impact case a) Dynamic case b) Equivalent static case

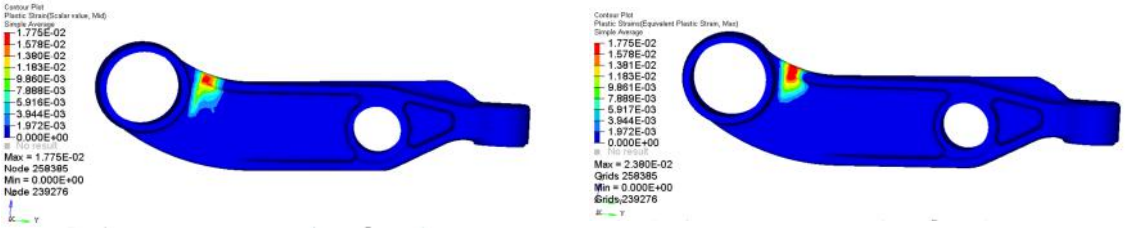

Figure 6.8: Plastic strain distribution- Kerb impact case a) Dynamic case b) Equivalent static case

6.3 Dynamic peak load and time period based study

A simplified model with coarser mesh of 3mm size was used to carry out the study on the effect of dynamic peak loads and time period of the impulse on the maximum displacement of the system discussed earlier in Fig 4.1. The simplification resulted in reducing the dynamic simulation time from 6 hours to an average of 30 min per model based on the time period of the impulse. The system was subjected a isosceles triangular impulse, as shown in fig 6.9.
Fig 6.9 based on the data presented in table 6.3 confirms the discussion in the previous chapter that the maximum dynamic effect is observed when the impulse duration equals the fundamental time period of the system (58ms in this case). The dynamic load factor drops below the maximum value when the impulse duration exceeds the fundamental time period of the system. Biggs (1964) has explained the significance of the time period of the impulse on the maximum response of the system. It was also observed that the value of the dynamic peak load had a negligible effect on the DLF.

Sl no.	t_d/T	DLF for varying dynamic peak loads in z-direction		
		15000 N	25000 N	35000 N
1	0.08	0.28	0.32	0.31
2	0.17	0.56	0.60	0.62
3	0.35	1.1	1.08	1.2
4	0.67	1.46	1.44	1.54
5	1	1.53	1.47	1.57
6	1.32	1.48	1.38	1.47
7	1.64	1.31	1.28	1.32
8	1.96	1.21	1.15	1.22

Table 6.3: Maximum displacement of the system subjected to isosceles triangular impulse for varying Dynamic peak load factor and duration

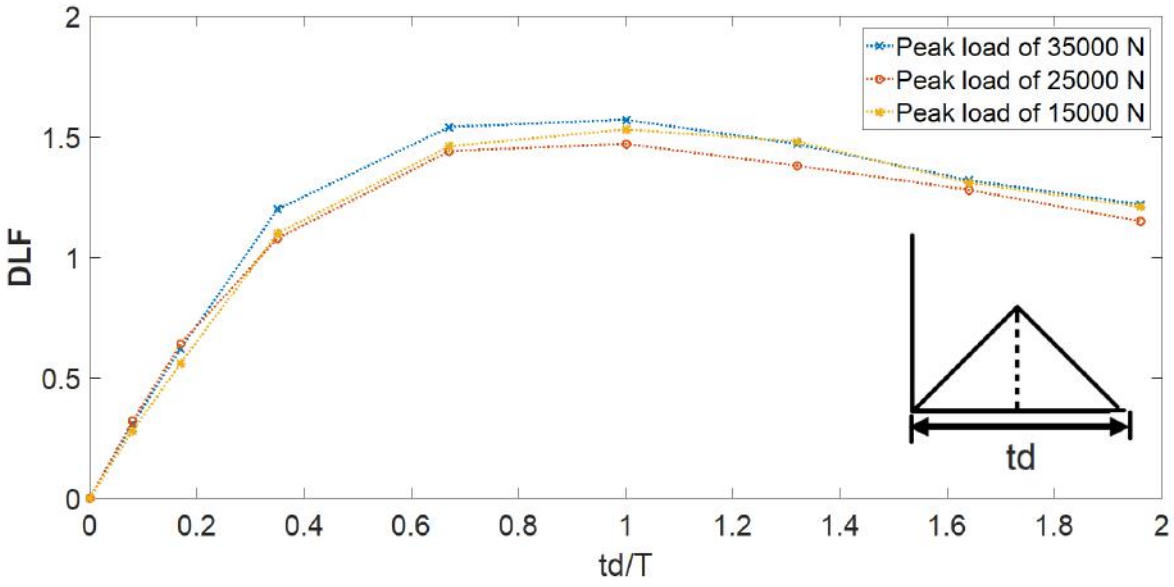

Figure 6.9: DLF vs ratio of impulse duration to fundamental time period of the system (t_d /T)

7
Final remarks

7.1 Conclusion

In this thesis work, a pre-study was conducted to investigate the effects of transient impulse loads on simple geometries such as the cantilever and the simply supported beams. The dynamic impact events were converted to equivalent static loads in the all the above cases. The response of the system was observed for various characteristics of loads such as duration of impulses, peak loads, shapes, loading rate etc. The physical properties of the beams were altered to study the effects on the response of the system too. The displacement response of the system was found to be governed predominantly by the time duration of the impulse loads. The fundamental i.e. the first eigen mode was the main contributor to the solution in all the cases. The effect of higher modes were observed as the impulse duration was considerably lower than the fundamental time period of the system. The deflection and the stress responses in both the beam configurations were found to match well from the dynamic study to the equivalent static case when load identification was adopted. The modal transient analysis was found to compliment the study well in understanding the active modes in the system.

Based on the results from the pre-study, a methodology for converting the dynamic loads to equivalent static loads was outlined. The methodology consists of 4 steps, which involves carrying out dynamic analysis and modal transient analysis of the component to understand the event and finally convert it to an equivalent static case. In the main study, the suspension assembly was studied to understand the response of the system for 2 load cases, namely pothole and side kerb impact load cases. The system identification through hyperstudy was found to be very sensitive to the loads and the bounds, thus leading to convergence at local optimum's. Modal transient analysis was found to be work well to identify the behaviour of the system and thus the loading directions. The scaling factor for the equivalent static loads was found to be dependent on the impulse duration's and the loading rates. Thus the equivalent static loads were identified for the tested load cases, which was found to vary between 1.27-1.58.

Some of the key findings of the study are :

- Understanding the global and local modes active in the system at the peak instant help in understanding the complexity of the load case and the ease of replication of stress and strain distribution in the equivalent static case as

shown in fig 6.4 & 6.7.

- For the cases considered in this study, we can do this conversion with confidence for the pothole load case. The stress and the strain results in equivalent static solution deviates from the dynamic event in case of the lateral kerb impact load case due to the occurrence of multiple active global and local modes at the peak instant.
- The maximum displacement of the system is majorly governed by the ratio of the impulse duration to the fundamental time period of the system in case of isosceles triangular impulse.
- For an isosceles triangular impulse, the maximum dynamic effect is observed when the duration of the impulse approximately equals the fundamental time period of the system Table 6.3.
- The dynamic peak load has negligible effect on the dynamic load factors as shown in fig 6.9.

7.2 Future work

Though the above studies were found to give good incites into the importance of the impulse characteristics and the equivalent static loads for various load cases and systems, some simplifications were done in obtaining the solutions, especilly in the assembly level system. Some of the improvements and studies that can be incorporated in further studies are:

- **Pre-tensioned springs in dynamic simulation**
  The dynamic simulations were found to be very sensitive to small changes due to which, the pre-tension in the spring were not considered in this. The dynamic models can be updated with the pre-tensioned spring to understand the behaviour of the system better.
- **Detailed bushing models**
  The static bushings models were modelled according to the dimensions of the housings to obtain reasonable outputs from the dynamic simulations. A more detailed bushing models with rate, amplitude and frequency dependencies included will help in understanding the system behaviour better as the load distribution in the components is highly dependent on the bushing models.
- **Path dependency studies**
  The stress in the bodies are path dependant, which might not be captured completely with equivalent static loads in complex loading scenarios . More detailed study on the path dependency can be carried out to arrive at the equivalent static loads.

Bibliography

[1] John M. Biggs. *Introduction to Structural Dynamics*. McGraw-Hill, Inc., 1964. ISBN: 978-0070052550.

[2] N.Ganesan P.K Roy. "Transient Response of a cantilever beam subjected to an impulse load". In: Academic press Limited, 1995, pp. 873–890. ISBN: ISBN 0022-460X95250873.

[3] Farzad Naeim. *The Seismic Design Handbook*. second edition. Springer Science+Business Media, LLC, 2003. ISBN: 978-1-4613-5681-3.

[4] Julian Happian-Smith. *An Introduction to Modern Vehicle Design*. Reed Educational and Professional Publishing, 2006. ISBN: 07506 5044 3.

[5] Roy R. Craig Jr. and Andrew J. Kurdila. *Fundamentals of structural dynamics*. second edition. John Wiley and Sons, Inc., 2006. ISBN: 978-0-471-43044-5.

[6] Sen Huang. "Dynamic analysis of assembled structures with nonlinearity". PhD thesis. Imperial College London, 2007.

[7] Anders Wirje and Kristian Carlsson. "Modeling and Simulation of Peak Load Events Using Adams - Driving Over a Curb and Skid Against a Curb". In: SAE International, 2011.

[8] Hampus Karlsson Sebastian Andersson. "Structural Response of Reinforced Concrete Beams Subjected to Explosions". Chalmers University of technology, 2012.

[9] K. Scott Smith Tony L. Schmitz. *Mechanical Vibrations*. Springer Science+Business Media, LLC, 2012. ISBN: 978-1-4614-0459-0.

[10] Shen R. Wu and Lei Gu. *Introduction to the Explicit Finite Element Method for Nonlinear Transient Dynamics*. John Wiley and Sons, Inc., 2012. ISBN: 978-0-470-57237-5.

[11] *ANSYS Structural Analysis Guide*. 2013.

[12] Siemens. *Basic Dynamic Analysis User's Guide*. 2014.

[13] M.V. Radchenko A.V. Sobolev. "Use of Johnson–Cook plasticity model for numerical simulations of the SNF shipping cask drop tests". In: 2016.

[14] *Altair Users Guide*. 2017.

[15] Kishen Chatra K. Vikranth Reddy Madhu Kodati. "A comprehensive kinematic analysis of the double wishbone and MacPherson strut suspension systems". In: ().

[16] Dassault Systems-Solid Works. "Understanding Nonlinear Analysis". In: Dassault Systems.

A

Appendix 1 - Pre-study on load identifiaction

Cantilever												
Sl No	Impulse load (N)	Impulse duration (ms)	Beam Dimensions LxBxH (mm)	Nodal Position (mm)		Nodal Displacement in Z direction (mm)	Optimized Nodal Displacements (mm)	Optimized Nodal Forces (N)	Max Beam Deflection - Analytical (mm)	Max Beam Deflection - FEM δdyn (mm)	Static Deflection of Beam δstat (mm)	Dynamic Load Factor = δdyn/δstat
1	750	8	500x100x20	0.25*L	125	-0.293952	-0.2939433	-177.9383	-3.27	-3.0243	-2.231	1.36
				0.5*L	250	-1.02293	-1.0229045	-373.8994				
				0.75*L	375	-1.98508	-1.9058341	-708.5032				
				L	500	-3.02443	-3.0243285	-427.383				
2	750	20	500x100x20	0.25*L	125	-0.3022	-0.302606	-101.4827	-3.58	-3.3309	-2.231	1.49
				0.5*L	250	-1.0763	-1.0776806	-168.1186				
				0.75*L	375	-2.1399	-2.1423116	-379.2322				
				L	500	-3.3282	-3.3309307	-807.9999				
3	500	4	500x100x10	0.25*L	125	-0.30285	-0.3028211	330.3504	-4.197	-5.9341	-11.9	0.50
				0.5*L	250	-1.44934	-1.4492509	592.1438				
				0.75*L	375	-3.47592	-3.4757464	-171.1224				
				L	500	-5.93412	-5.9338584	-351.5969				
4	500	20	500x100x10	0.25*L	125	-2.04829	-2.0482478	-161.9876	-19.68	-21.2965	-11.9	1.79
				0.5*L	250	-7.16503	-7.1647291	-290.2485				
				0.75*L	375	-13.9466	-13.946342	-632.1526				
				L	500	-21.2965	-21.296503	-385.6412				
Simply Supported												
1	1000	8	750x100x10	0.2*L	150	-3.23468	-3.2344599	-165.8076	5.1	-5.5516	-5.13	1.08
				0.4*L	300	-5.2741	-5.2737584	-358.3645				
				0.5*L	375	-5.55164	-5.5512557	-236.828				
				0.6*L	450	-5.27007	-5.2696939	-338.5411				
				0.8*L	600	-3.23025	-3.230001	-169.2375				
2	1000	12	750x100x10	0.2*L	150	-4.47555	-4.4759216	-376.8832	7.19	-7.6134	-5.13	1.48
				0.4*L	300	-7.24139	-7.2411823	-465.144				
				0.5*L	375	-7.61344	-7.6126013	-191.4537				
				0.6*L	450	-7.23929	-7.2391939	-451.678				
				0.8*L	600	-4.47408	-4.4742665	-381.5322				
3	750	4	1000x100x10	0.2*L	200	-1.57097	-1.5709642	430.8974	3.4	-3.2245	-9.146	0.35
				0.4*L	400	-2.98969	-2.9896553	-221.309				
				0.5*L	500	-3.22458	-3.2245269	-337.3076				
				0.6*L	600	-2.98964	-2.9895937	-221.2096				
				0.8*L	800	-1.57092	-1.570887	430.87				
4	750	12	1000x100x10	0.2*L	200	-5.08646	-5.0870223	-169.826	9.11	-8.6694	-9.146	0.95
				0.4*L	400	-8.24133	-8.2422771	-214.9773				
				0.5*L	500	-8.66841	-8.669426	-114.9632				
				0.6*L	600	-8.24046	-8.2414579	-214.788				
				0.8*L	800	-5.08501	-5.0856166	-168.8757				

Table A.1: Results - Load identification for the displacements

Cantilever							
Sl No	**Impulse load (N)**	**Impulse duration (ms)**	**Beam Dimensions LxBxH (mm)**	**Length along the beam (mm)**		**Element Von Mises Stress-Dynamic (MPa)**	**Optimized Element Von Mises Stress (Mpa)**
1	750	8	500x100x20	0	0	63.38	57.85
				0.25*L	125	43.27	43.1
				0.5*L	250	21.88	22.49
				0.75*L	375	6.16	6.69
2	750	20	500x100x20	0	0	62.61	58.66
				0.25*L	125	47.05	47.01
				0.5*L	250	28.67	28.47
				0.75*L	375	12.26	11.81
3	500	4	500x100x10	0	0	14.96	15.43
				0.25*L	125	28.22	29.04
				0.5*L	250	31.53	31.85
				0.75*L	375	15.13	14.87
4	500	20	500x100x10	0	0	160.1	158.5
				0.25*L	125	99.12	102.4
				0.5*L	250	53.11	55.69
				0.75*L	375	16.09	21.02
Simply Supported							
1	1000	8	750x100x10	0.2*L	150	27.59	27.95
				0.4*L	300	49.25	48.72
				0.5*L	375	52.21	51.71
				0.6*L	450	49.36	48.88
				0.8*L	600	26.73	28.68
2	1000	12	750x100x10	0.2*L	150	42.04	40.83
				0.4*L	300	65.57	65.81
				0.5*L	375	67.77	68.71
				0.6*L	450	64.43	66.1
				0.8*L	600	42.79	41.93
3	750	4	1000x100x10	0.2*L	200	2.17	1.89
				0.4*L	400	19.06	20.3
				0.5*L	500	23.88	25.3
				0.6*L	600	19.48	20.8
				0.8*L	800	1.92	1.71
4	750	12	1000x100x10	0.2*L	200	25.78	25.85
				0.4*L	400	41.66	42.1
				0.5*L	500	43.75	44.16
				0.6*L	600	41.19	42.35
				0.8*L	800	25.73	26.38

Table A.2: Results - Load identification for von-mises stress